# Prevalence and immune modulator role of the *peg344 gene* among Hypervirulent *Klebsiella pneumoniae*

by

Güz Ekinci

A Dissertation Submitted to the
Graduate School of Health Sciences

in Partial Fulfillment of the Requirements for

the Degree of

Master of Science

in

Medical Microbiology

KOÇ
ÜNİVERSİTESİ

# Prevalence and immune modulator role of the *peg344* gene among Hypervirulent *Klebsiella pneumoniae*

Koç University

Graduate School of Health Sciences

This is to certify that I have examined this copy of a master's thesis by

Güz Ekinci

and have found that it is complete and satisfactory in all respects,
and that any and all revisions required by the final
examining committee have been made.

Committee Members:

Prof. Dr. Füsun Can (Advisor)

Prof. Dr. Önder Ergönül

Prof. Dr. Özgen Eser Köseoğlu

Date: August 1, 2023

# ABSTRACT


## Prevalence and immune modulator role of the *peg344* gene among Hypervirulent *Klebsiella pneumoniae*

Güz Ekinci

Master of Science in Medical Microbiology

August 1, 2023

Hypervirulent *Klebsiella pneumoniae* (hvKp) is an emerging pathogen threatening healthy and immunocompromised patients. Since hvKp first appeared in Taiwan in 1986, its prevalence has increased drastically around the globe. Yet, there is no study focusing on hypervirulent strains in Turkey. *peg344, iutA, and iroB* are the highly accurate biomarker genes for hypervirulence. However, the pathogenesis mechanism of the *peg344* putative metabolite transporter is still unclear. This study aims to elucidate the hypervirulence surveillance in Turkey and to understand the immune modulator role of the *peg344* gene *in vivo* and *in vitro* infection models. In total, 230 *K.pneumoniae* isolates isolated from ten different healthcare centers in Turkey between January 2015 to March 2023 were included in the study. All strains were screened for hypervirulence genes *peg344, iutA, and rmpA.* The isolates harboring at least two of the hypervirulence gene were categorized as hypervirulence gene *K.pneumoniae*. The isolates which exhibited a hypermucoviscous phenotype in string test or virulent phenotype in 48-hour *C.elegans* fertility assay were classified as hypervirulent. The hypervirulence prevalence between 2022-2023 was significantly higher than 2017-2018 ($p=0.024$), and 2015-2016 ($p<0.0001$). The most prominent ST types were ST2096, and ST23 (30.77% and 23.08% respectively); K1 and K2 were the most common capsule serotypes among the hypervirulent cohort (46.15% and 15.38% respectively). THP-1-driven macrophage cells were infected with selected isolates including cKp, hgKp, hvKp, and Δ*peg344*-mutant isolates. hvKp isolates had decreased the viability of macrophages (from 91.5% to 81.5%) and increased the M2 convergence ratio at 2 hours of infection. Macrophages could inhibit the cKp isolates, but hvKp isolates were able to grow inside the macrophages at 3 hours of infection. Also, hvKp infection secreted less TNFα than cKp infection (368, 1462 pg/mL respectively). The *peg344* deletion decreased the bacterial growth (from 430% to -3%) within the macrophages and recovered the TNFα secretion levels (from 203 to 824 pg/mL).

In conclusion, hypervirulent *K.pneumoniae* is an emerging pathogen, and a serious concern in our region just like in other parts of the world. The *peg344* gene is an accurate biomarker for differentiation in this region. The hypophagia of macrophages and the suppressed proinflammatory responses in the early stages contributes to the severe infections caused by hypervirulent clones. The *peg344* gene plays an important role in bacteria's resistance against phagocytosis by macrophage cells.



**Keywords:** Hypervirulent, *Klebsiella pneumoniae, peg344* gene, hypervirulence genes, epidemiology, string test, *C.elegans* fertility assay, *in vitro* macrophage infection assay, hypophagia

# ÖZETÇE

## *peg344* geninin Hipervirülan *Klebsiella pneumoniae*'deki Yaygınlığı ve İmmün Modülatör Rolü

Güz Ekinci

Tıbbi Mikrobiyoloji, Yüksek Lisans

1 Ağustos 2023

Hipervirülan Klebsiella pneumoniae (hvKp), sağlıklı ve bağışıklığı baskılanmış hastaları tehdit eden, gelişmekte olan bir patojendir. hvKp ilk olarak 1986'da Tayvan'da ortaya çıktığından beri, yaygınlığı tüm dünyada büyük ölçüde artmıştır. Ancak Türkiye'de hipervirülan suşlara odaklanan bir çalışma bulunmamaktadır. *peg344, iutA ve iroB,* hipervirülans için önemli biyobelirteç genlerdir. Bununla birlikte, *peg344* varsayılan metabolit taşıyıcısının patogenez mekanizması hala belirsizdir. Bu çalışma, Türkiye'deki hipervirülans sürveyansını aydınlatmayı ve *peg344* geninin *in vivo* ve *in vitro* enfeksiyon modellerindeki immün modülatör rolünü anlamayı amaçlamaktadır. Ocak 2015-Mart 2023 tarihleri arasında Türkiye'deki on farklı sağlık merkezinden izole edilen toplam 230 *K.pneumoniae* izolatı çalışmaya dahil edilmiştir. Tüm suşlar hipervirulans genleri *peg344, iutA ve rmpA* için taranmıştır. Hipervirülans genlerinin en az ikisini barındıran izolatlar, hipervirülans geni *K.pneumoniae* olarak kategorize edilmiştir. Uzama testinde hipermukoviskoz fenotip veya 48 saatlik *C.elegans* fertilite testinde virülan fenotip gösteren izolatlar hipervirülan olarak sınıflandırılmıştır. 2022-2023 yılları arasındaki hipervirülans yaygınlığı, 2017-2018 ($p=0,024$) ve 2015-2016'ya ($p<0,0001$) göre anlamlı derecede yüksek bulunmuştur. Hipervirülan izolatlar arasındaki en belirgin ST tipleri ST2096 ve ST23 (sırasıyla %30,77 ve %23,08), ve en yaygın kapsül serotipleri ise K1 ve K2 (sırasıyla %46.15 ve %15.38) olarak bulunmuştur. THP-1 hücrelerinden dönüştürülen makrofajlar; cKp, hgKp, hvKp ve Δpeg344-mutant izolatlarından seçilmiş örneklerle enfekte edilmiştir. Enfeksiyonun 2. saatinde hvKp izolatları, makrofajların canlılığını azaltmış (%91,5'ten %81,5'e) ve M2 dönüşüm oranını artırmıştır. Makrofajlar cKp izolatlarını inhibe edebilmiş, ancak hvKp izolatları, enfeksiyondan 3 saat sonra makrofajların içinde büyüyebilmiştir. Ayrıca makrofajlar hvKp enfeksiyonunda, cKp enfeksiyonundan daha az TNFα salgılamıştır (sırasıyla 368 ve 1462 pg/mL). *peg344* geninin silinmesi, makrofajlar içindeki bakteri üremesini (%430'dan -%3'e) azaltmış ve TNFα salgılama düzeyini (203'ten 824 pg/mL'ye) geri kazandırmıştır.

Sonuç olarak, hipervirülan *K.pneumoniae* gelişmekte olan bir patojendir ve dünyanın diğer bölgelerinde olduğu gibi ülkemizde de ciddi bir tehlikedir. *peg344* geni, bu bölgede karakterizasyon için doğru bir biyobelirteçtir. Makrofajların hipofajisi ve erken evrelerde bastırılmış proinflamatuar yanıtlar, hipervirülan klonların neden olduğu ciddi enfeksiyonlara katkıda bulunur. *peg344* geni, bakterilerin fagositoza karşı direncinde önemli bir rol oynar.

**Anahtar Kelimeler:** Hypervirülan, *Klebsiella pneumoniae, peg344* geni, hypervirülans genleri, epidemiyoloji, uzama testi, *C.elegans* fertilite testi, *in vitro* makrofaj enfeksiyon testi, hipofaji

# ACKNOWLEDGEMENTS

First and foremost, I would like to express my sincere gratitude to my thesis advisor **Prof. Dr. Füsun Can.** In this Master's journey that I had started as a scientist-to-be, she taught me how to be a researcher. She always listened and supported my ideas, and gave many great advice which has resulted in the making of this thesis project. I am thankful that I had the chance to share the great wisdom and experience of Prof. Dr. Füsun Can.

Secondly, I would like to thank **Prof. Dr. Önder Ergönül.** He has a great model of how to be a great researcher and a great colleague. Even on his busiest day, he didn't forget to put smiles on anybody around him. I am grateful to have listened to Prof. Dr. Ergönül's exquisite stories.

Also, I would like to thank **Assistant Prof. Özlem Doğan** who had interested in my findings in every Monday meeting and gave her valuable advice so that I wouldn't get lost along the way.

My sincere gratitude is to **my great colleagues at KUISCID.** During my Master's I had many friends from whom I had the opportunity to share their experiences, and learned how to be a team member. I am also thankful to my colleagues for their intellectual, experimental, and emotional contributions. Even on the most stressful days of KUISCID, I had shared many laughs with my friends for which I am thankful.

Last, but not least, I am sincerely grateful to **my loving parents, and sister.** It has been a long journey searching for my passion during which they have always supported me. I will be lucky to have their love and support along the way ahead of me.

TABLE OF CONTENT

LIST OF TABLES

LIST OF FIGURES

# ABBREVIATIONS

| | |
|---|---|
| AmpR | Ampicillin Resistance Gene |
| AMR | Antimicrobial Resistance |
| ARA | L-arabinose |
| ATCC | The American Type Culture Collection |
| CarR | Carbapenem Resistant |
| CEV | *C.elegans* virulence score |
| cKp | Classical *Klebsiella pneumoniae* |
| ColR | Colistin Resistant |
| CR | Chloramphenicol Resistance Gene |
| DMT | Drug/Metabolite transporter |
| DNA | Deoxyribonucleic Acid |
| ELISA | Enzyme-Linked Immunosorbent Assay |
| CD | Cluster of Differentiation |
| IL | Interleukin |
| TNFα | Tumor Necrosis Factor α |
| FACS | Fluorescence-Activated Cell Sorting |
| FBA | Fructose-1, 6-Bisphosphate Aldolase |
| GmR | Gentamicin Acetyltransferase |
| hgKp | Hypervirulence Gene *Klebsiella pneumoniae* |
| hvKp | Hypervirulent *Klebsiella pneumoniae* |
| kB | Kilobase |
| LB | Luria Broth |
| MDR | Multidrug Resistant |
| MIC | Minimum Inhibitory Concentration |
| MLST | Multiple Locus Sequence Typing |
| NCBI | National Center for Biotechnology Information |
| NGM | Nematode Growth Medium |
| OD | Optical Density |
| PBS | Phosphate Buffered Saline |
| PCR | Polymerase Chain Reaction |
| PMA | Phorbol 12-Myristate 13-Acetate |
| RPM | Revolutions per Minute |

| | |
|---|---|
| SDS | Sodium Dodecyl Sulfate |
| SP-A | Surfactant Protein A |
| ST | Sequence Type |
| $T_M$ | Melting Temperature |
| TLR | Toll-like Receptors |
| TSA | Tryptic Soy Agar |
| *Λ*RED | Lambda Red Recombination |

# CHAPTER 1:

# INTRODUCTION

## 1.1 *Characteristics of Classical and Hypervirulent Klebsiella pneumoniae*

*Klebsiella pneumoniae* emerges as an important clinical and public health threat worldwide due to the severe infections, causing pneumonia, liver abscess, soft tissue and surgical wound infections, urinary tract infections, meningitis, endophthalmitis, bloodstream infections, and sepsis in patients with the weakened immune system, who are admitted to chemotherapy or to immunosuppressive treatment. (Turton et al. 2017; Brisse et al., 2019) This great infection ability can be explained by their capacity to endure hunger, to exchange DNA easily with other members of the human microbiome, their natural antibiotic resistance mechanisms, and their highly competitive ability. (Moellering et al., 2010; Paczosa et al. 2016)

In recent years, a novel more destructive variant has emerged, hypervirulent *Klebsiella pneumoniae* (hvKp). hvKp infections have higher mortality and morbidity rate compared to classical *Klebsiella pneumoniae* (cKp). (Russo et al., 2019) The mechanism of enhanced pathogenicity of this variant is not yet fully understood. Also, the differentiation of hypervirulent from classical strains is not yet decided in the literature. (Harada et al., 2018)

Hypervirulent *Klebsiella pneumoniae* differs from classic *K.pneumoniae* infections in the means of phenotype, genotype, clinical course, and also, recognition by clinicians. HvKp has emerged as a community-acquired infection. This emerging pathogen can infect any part of the body in healthy individuals at any age. (Melot et al., 2016; Cheng et al., 2012; Jung et al., 2015; Prokesch et al., 2016) Another important feature of hvkP is that it can spread metastatically to more than one area in infected patients. (Cheng et al., 1991; Russo et al., 2012) Pyogenic liver abscess is the most prominent clinical syndrome of hvKp infections. (Wang et al., 1998) However, it has been reported that hvKp can infect almost every part of the body and cause non-hepatic abscesses, pneumonia, necrotizing fasciitis, endophthalmitis, and meningitis. (Russo et al., 2019) Even though this feature of hvKp is

not seen in cKp infections, it is encountered in infections caused by other members of the Enterobacteriaceae family. (Shi et al., 2017)

### 1.2 *Epidemiology of Hypervirulent Klebsiella pneumoniae*

Hypervirulent *Klebsiella pneumoniae* was first identified in a case series published in Taiwan in 1986. In this case series, community-acquired liver abscesses caused by hvKp have been reported in healthy patients with severe concomitant end-organ manifestations such as meningitis and endophthalmitis. (Liu et al., 1986) Sporadic spread of hvKp has been observed in many Asian, European, and American countries since the first case series reports in Taiwan. (Zhang et al., 2016; Russo et al., 2019) *Klebsiella pneumoniae* liver abscess, which is considered an epidemic disease in Asian countries, is detected at a high rate in China, South Korea, and our neighboring countries, Iran. The annual incidence of liver abscesses in Taiwan caused by hvKp increased by almost 60% between the years 1996 and 2004. (Hsieh et al., 2008) In South Korea, the rate of liver abscess caused by *K.pneumoniae* was 3.3% in the 1970s, whereas it has been observed at 78.2% in the mid-2000s. (Chung et al., 2007) The rapid conversion of the cKp to hvKp is concerning. In a study covering 105 countries, it was shown that the rate of carbapenem-susceptible-hvKp, which was 0.4% in 1980, increased to 27.03% in 2022. (Wu et al., 2022) Hence, the prevention and treatment of the spread of infections caused by bacteria with multidrug resistance and hvKp profile are among the priority issues. As a general distribution, it has been reported that the incidence of hvKp is 90% in Asian countries (El Fertas-Aissani et al. 2013; Peirano et al. 2013; Pereira et al., 2015) In a China-based study, mortality in the bloodstream infections due to hvKp was reported as 37-42%, while this rate was found to be 56.2% in India. (Russo et al., 2019) In a study conducted in Iran, 60.95% of *K.pneumoniae* isolates collected from various patients were shown to be hypervirulent. (Zamani et al., 2013) Currently, there is no report indicating the prevalence of hvKp strains in Turkey. There is an urgent need to distinguish between hypervirulent and classical strains clinically, phenotypically, and genotypically.

## 1.3 *Differentiation of Hypervirulent Klebsiella pneumoniae*

### 1.3.1 *Clinical Differentiation of Hypervirulent Klebsiella pneumoniae*

Hypervirulent strains can be distinguished from cKp by clinical features. The most significant among these features is the ability of hvKp to cause severe infections in both immunocompromised and healthy individuals. (Melot et al., 2016; Cheng et al., 2012) Secondly, it has been observed that hvKp tends to metastasize and spread to different regions where they trigger diseases in different regions including endophthalmitis, necrotizing fasciitis, meningitis, and bacteremia, regardless of the site of infection. (Cheng et al., 1991; Russo et al., 2012)

### 1.3.2 *Phenotypic Differentiation of Hypervirulent Klebsiella pneumoniae*

The phenotypic differentiation of hypervirulent strains is based on hypermucoviscosity. Hypermucoid phenotype has been accounted as a predictor of hypervirulence back when hvKp began to appear. (Fang et al., 2004; Russo et al., 2019) In recent years, it has been determined that hypermucoviscosity is associated not only with hypervirulent strains. (Russo et al., 2021) Also, not all hypervirulent strains exhibit the hypermucoviscous phenotype. (Catalán-Nájera et al., 2016) This phenotype is tested by string test which is a semi-sensitive method from the early periods.

### 1.3.3 *Genotypic Differentiation of Hypervirulent Klebsiella pneumoniae*

Virulence factors are the main criteria for the genotypic differentiation of hvKp. Enhanced virulence profiles make hvKp strains more pathogenic compared to cKp. (Russo et al., 2019) There are several important virulence factors associated with hypervirulence such as capsule serotypes, siderophores, hypermucoviscosity regulation, *peg344* gene, and fimbriae. (Russo et al., 2018) Among these genotypic features; hypermucoviscosity, siderophore, and *peg344* genes are well-studied among hypervirulent strains.

***Capsule Serotypes***

Capsule serotypes are important virulence factors that enable the bacteria to evade phagocytosis and to adhere stronger to the tissues. *K.pneumoniae* has 134 different capsule serotypes. K1 and K2 capsule serotypes are mostly seen in hvKp, and these serotypes are generally associated with the hypervirulent phenotype. (Zhu et al., 2021; Du et al., 2022) In China, 42.9% of clinical isolates of hypermucoviscous *K.pneumoniae* associated with various invasive infections, including pyogenic liver abscess, had the K2 serotype and 23.8% had the K1 serotype. (Russo et al., 2019)

HvKp strains with K1 and K2 capsule serotypes are more resistant to phagocytosis and intracellular killing by macrophages and neutrophils, compared to strains with other serotypes, regardless of their hypermucoviscosity properties. (Wanford et al., 2021) Different microbiological and immunological reasons cause the pathogenicity of K1 and K2 strains to be higher than other strains. Firstly, K1 and K2 capsule serotypes lack specific mannose repeats that allows recognition by host factors such as mannose-binding receptors on macrophage and lung-secreted surfactant protein A (SP-A) K1 and K2 capsule serotypes affect the immune response of the host against the bacteria. (Kabha et al., 1995; Sahly et al., 2008) Studies showed that capsule serotypes K1 and K2 lack mannose and rhamnose, and can be recognized by macrophage lectin receptors to induce phagocytosis. (Athamna et al., 1991; Fung et al., 2002)

Secondly, K1 and K2 capsules contain sialic acid, a host-specific monosaccharide, on their surface that mimics host cells, thereby enabling host immune cells to escape. (Lee et al., 2013) In addition, sialic acid has been shown to contribute to the formation of the hypermucoviscous phenotype and therefore, directly or indirectly, is responsible for the anti-phagocytic activity. (Lee et al., 2013) In another study, fructose-1, 6-bisphosphate aldolase (FBA), which is one of the surface proteins, was detected in hvKp strains with the K1 serotype. The expression of this protein has been found to protect bacteria against neutrophils. (Lee et al., 2020)

Lastly, K1 and K2 strains have more diverse O serotypes than strains with other K serotypes (Follador et al., 2016), which may help K1 and K2 strains evade host immune systems. These strains also cause less reactive oxygen release by neutrophils than strains

with other serotypes, allowing better survival in human tissues. (Paczosa et al., 2016; Sahly et al., 2004)

Virulence genes can be found in both plasmid and chromosomal DNA. The genes involved in capsule production are located in the capsular polysaccharide synthesis (*cps*) region of the chromosome. (Arakawa et al.1995; Fang et al., 2010) magA (*K1_wzy*) gene, encoded in the cps region, plays an important role in capsular polysaccharide synthesis required for hypermucoviscous phenotype and resistance to complement-mediated lysis. *rmpA* and *rmpA2* genes are the regulators known to be required for the hypermucoviscous phenotype in hvKP strains. Both *rmpA* and *rmpA2* can be carried by plasmid or chromosome; chromosomal *rmpA* (*c-rmpA*) is seen in ICEKp1, an integrative and conjugative element. However, plasmid-borne *rmpA* is the most common. (Paczosa et al., 2016; Yu et al., 2006).

***Siderophores***

Siderophore proteins are competing bacterial proteins for chelating iron molecules from the environment and the host. (Paczosa et al., 2016) Iron is one of the most important elements for both the human body and bacterial cells. (Russo et al., 2014) Bacteria can not easily get iron molecules due to the low solubility of iron and competition with the host's iron-binding proteins under stress conditions such as infection. The low extracellular density of iron, which is the most essential mineral for many metabolic processes, enables bacteria to turn into an immune system defense by using alternative routes for the iron uptake process. (Lee et al., 2017) In *K.pneumoniae*, siderophore structures can bind iron molecules with a higher affinity than the host cell during the iron uptake process. Hence, *K.pneumoniae* gets the upper hand in the battle for iron during the infection process. (Wang et al., 2020)

Siderophores are small iron-binding molecules that are synthesized inside the bacterial cell and secreted out of the cell. When secreted, siderophores bind to the surrounding iron and transport it back to the cells. Subsequently, the iron-siderophore complexes are recognized by the outer membrane receptors and taken up into the periplasm. (Paczosa et al., 2016) Then, the iron-siderophore complexes, which are transported to the cytoplasm by specific transport systems, release the ferric iron form into the cytoplasm so that

bacteria could metabolize the iron. (Hsieh et al., 2008) When the siderophore protein releases the ferric iron into the cytoplasm, it is recirculated back into the periplasm so that it can be secreted and bind to more iron molecules in the environment. (Russo et al., 2014)

Several studies have shown that hvKp produces 6 to 10 times more siderophores when compared to cKp. (Russo et al., 2014; Russo et al., 2018) There are four different siderophore systems in hvKp strains, including enterobactin, yersiniabactin, salmochelin, and aerobactin. It has been determined that siderophore production also increases the growth of bacteria in addition to providing iron uptake. (Paczosa et al., 2016; Russo et al. 2015; Russo et al. 2016)

Enterobactin is produced by more than 90% of Enterobacteriaceae isolates. (Raymond et al., 2003) The three catechol rings in the enterobactin structure provide the highest iron binding capacity for both cKP and hvKP among the four different siderophore systems. However, enterobactin can not ensure the survival of the bacterial cell alone for both cKp and hvKp. Host cells produce the antimicrobial siderophore-binding lipocalin-2 to directly kill the pathogen. (Holmes et al., 2005) Studies have shown that *Klebsiella pneumoniae* isolates producing only enterobactin fail to grow as a result of lipocalin-2 binding. (Bachman et al. 2012). Therefore, producing alternative siderophores increases the survival chances of *K.pneumoniae* isolates. In other words, strains containing salmochelin and yersiniabactin survive in the presence of lipocalin-2. (Bachman et al., 2012; Holden et al., 2014)

Yersiniabactin is originally produced by yersinia species. These species transfer the yersiniabactin locus which is located on the pathogenicity island via horizontal gene transfer. (Bach et al., 2000) Yersiniabactin siderophore is an important virulence factor for the pathogenesis of cKp strains in mouse models. (Russo et al., 2014) Also, the gene clusters encoding for yersiniabactin and aerobactin are more prevalent in hvKp than ckP strains. (Hsieh et al., 2008) However, the pathogenesis of yersiniabactin in hvKp infections is still unclear.

The genes encoding aerobactin and salmochelin are located on a large virulence plasmid (pLVPK) that is absent in most cKP strains. (Nassif et al., 1986; Struve et al., 2015) Therefore, while aerobactin and salmochelin are rarely found in cKP strains, they are

found widely in hvKP isolates. (Wang et al., 2000; Russo et al., 2018) Aerobactin, encoded by the iucABCD operon, is the most basic siderophore system of hvKp, which performs iron uptake via the iutA receptor located on the outer membrane. (Russo et al., 2014) In many studies, the presence of the *iucABCD-iutA* operon system has been reported higher in hvkP compared to cKp. (Yu et al., 2006; Lee et al., 2017) In a study conducted by Yu and his colleagues, it was shown that hvKp isolates harboring rmpA and *iucABCD-iutA* genes had seriously high fatality due to high virulence in an in vivo mouse model, regardless of the capsule type. (Yu et al., 2008) Aerobactin, unlike other siderophores, contributes to the infection in the mouse model of hvKp, and in addition, it enables the bacterium to maintain its viability in human acid fluid or serum. Therefore, aerobactin is one of the most important virulence factors of hvKp. (Wang et al., 2000; Russo et al., 2014; Russo et al., 2015) Besides, aerobactin is responsible for >90% of the siderophore activity in hvKp infections where the strain has all four different siderophore systems. (Russo et al., 2014)

Aerobactin contributes to the activation of different virulence factors in addition to iron uptake systems. (Russo et al., 2014) For example, the presence of iron in the environment provides *rmpA* activation. Hence, there is a tight link between *rmpA* and aerobactin in hypervirulent *Klebsiella pneumoniae*.

***peg344 gene***

The *peg344* gene has been detected in the virulence plasmid of a hvKp strain whose complete genome and transcriptome analysis has been completed based on increased RNA abundance of the *peg344* gene when grown in human ascites fluid. (Bulger et al., 2017) Although the exact function of the gene is unknown, as a result of homology modeling, it has been determined that it encodes a metabolite transporter located in the inner membrane. It has also been reported that it acts as a permease enzyme from drug/metabolite (DMT) transporter families. (Russo et al., 2018) In Bulger's study, several metabolites have been tested with *peg344* harboring strain whether the metabolites are being transported or not in order to assign a candidate metabolite for this transporter. They have concluded that this protein does not transport amino acids, L-rhamnose, and rhamnolipids. In the same study, silencing of the *peg344* gene significantly decreased the survival of mice compared to the survival of mice infected with *peg344*

harboring wild-type strains. On top of that, the presence of *peg-344* detected in hvKp isolates was observed to cause pneumonia in subcutaneous infection CD1 mouse models, while systemic infection was not observed. (Bulger et al., 2017)

## 1.4 *Hypervirulence Biomarkers*

### 1.4.1 *Phenotypic Biomarkers of Hypervirulence*

Several strategies for hypervirulent differentiation are based on phenotype such as colony morphology analysis, string test, serum killing assay, nematode or mice survival assays, and quantitative siderophore assay. (Shi et al., 2018) However, these phenotypic strategies on their own can miss some of the hypervirulent strains which exhibit different virulent profiles. One hypervirulent strain can cause high mortality in a mouse model, but should not exhibit hypermucoviscosity. Therefore, a combination of phenotypic assays should be tested on hypervirulent differentiation. (Russo et al., 2018; Du et al., 2022)

### 1.4.2 *Genotypic Hypervirulence Biomarkers*

In a study published in 2018, Russo and his colleagues identified five biomarker genes for hypervirulent strains including *iroB* (salmochelin siderophore synthesis gene), *iucA* (aerobactin siderophore synthesis gene), *rmpA*, and *rmpA2* (regulator genes of hypermucoviscous phenotype). The *peg344* gene was identified as the biomarker gene with the highest accuracy for hypervirulence differentiation, with an accuracy of 97%. (Russo et al., 2018)

Considering all this knowledge on enhanced virulence capacity and the associated high morbidity rate of hypervirulent *Klebsiella pneumoniae* strains (Russo et al., 2019), it is crucial to detect the surveillance of hvKp strains in Turkey since it is a region with high antimicrobial resistance rates. Also, it is critical to elaborate on the limited pathogenesis mechanism of the *peg344* metabolite transporter. (Harada et al., 2018) Therefore, the main goal of this thesis project is to elucidate the prevalence of hvKp strains and the pathogenesis mechanism associated with the *peg344* metabolite transporter.

# CHAPTER 2

# MATERIALS and METHODS

## 2.1 *Study Population*

In total 230 *K.pneumoniae* isolates from the patients diagnosed with *Klebsiella pneumoniae* infection between January 2015 and March 2023 were included in this study. The strains were collected from ten different healthcare centers from Istanbul, Ankara, and Denizli. Antimicrobial resistance to carbapenems and colistin were recorded. This study was approved by the Koç University Ethical committee, the protocol number is 2023.231.IRB2.051.

## 2.2 *Virulence Gene Screening by Conventional PCR*

Total DNA extraction of each isolate was done with a commercial extraction kit (QIAGEN DNeasy UltraClean Microbial Kit, U.S.). After growing overnight on a TSA plate (Becton, Dickinson and Company, U.S.) at 37℃, a loop of colonies (1 µL) was picked from fresh cultures grown overnight at 37℃. Loopful colonies were placed within the tubes containing Powerbeads, 300 µL Powerbead solution, and 50 µL lysis buffer. The tubes were vortexed horizontally at maximum speed for 10 minutes and centrifuged for 30 seconds at 10,000 g. The supernatant was mixed with 100 µL of IRS solution and incubated at 4℃ for 5 minutes. The mixture was centrifuged at 10,000 g for 30 seconds and the supernatant was placed in a filtered collection tube. The filtered collection tube was centrifuged at 10,000 g for 30 seconds and flow-through was discarded. 700 µL of wash buffer was added to the filtered collection tube and centrifuged for 30 seconds at 10,000 g. Flow-through was discarded and the filtered tube was centrifuged again for 2 minutes at 10,000 g. The filter is placed onto a new collection tube and 50 µL of elution buffer was added to the filter. The collection tube was centrifuged for 30 seconds at 10,000 g and the elution was stored at -20℃. The concentrations of the DNA solutions were measured with a Nanodrop 2000 Spectrophotometer (Thermo Scientific, US); $A_{260/230}$, $A_{260/280}$ values were also determined.

DNA samples were used for conventional PCR for screening the virulence genes *peg344, iutA, rmpA, magA, K2, K5, fimH, kfu, ybtS, entB, allS, wabG, fyuA, mrkD* following a previous protocol with slight modifications. (Dogan et al., 2021) Primer sequences and reaction temperatures were listed in Table 2.1. DreamTaq Green PCR master mix (Thermo Fisher Scientific, US) was used for the PCR reactions. 12.5 µL of DreamTaq Green PCR master mix was supplemented with 0.5 µL 25 pmol forward primer, 0.5 µL 25 pmol reverse primer, 11 µL of nuclease-free water, and 0.5 µL DNA sample. For only the *peg344* PCR reaction, 5.5 µL of betaine was used with 5.5 µL of nuclease-free water. The PCR reaction was done with the conditions; initial denaturation at 94°C, 5 min., 30 cycles of denaturation at 94°C, 25 sec., annealing at the corresponding melting temperature stated in Table 2.1., 40 sec., extension at 72°C, 50 sec. and final extension at 72°C, 6 min. 5 µL of PCR products were run in 1.5% agarose gel for 40 minutes at 90V.

Table 2.1: Sequences and melting temperatures of primers used for virulence screening.

| **Name of the gene** | **$T_M$ (℃)** | **Forward Primer Sequence** | **Reverse Primer Sequence** | **Source** |
|---|---|---|---|---|
| *peg344-PP1* | 61 | CTTGAAACTATCCCTCCAGTC | CCAGCGAAAGAATAACCCC | Russo et al., 2018 |
| *peg344-PP2* | 61 | AAAGGACAGAAAGCCAGTG | CAATGACGAGGGGGATAATC | |
| *iutA* | 60 | GGGAAAGGCTTCTCTGCCAT | TTATTCGCCACCACGCTCTT | Compain et al., 2014 |
| *K2* | 50 | CAACCATGGTGGTCGATTAG | TGGTAGCCATATCCCTTTGG | |
| *kfu* | 60 | GGCCTTTGTCCAGAGCTACG | GGGTCTGGCGCAGAGTATGC | |
| *ybtS* | 60 | GACGGAAACAGCACGGTAAA | GAGCATAATAAGGCGAAAGA | |
| *entB* | 60 | GTCAACTGGGCCTTTGAGCCGTC | TATGGGCGTAAACGCCGGTGAT | |
| *allS* | 65 | CATTACGCACCTTTGTCAGC | GAATGTGTCGGCGATCAGCTT | |

| | | | | |
|---|---|---|---|---|
| *mrkD* | 58 | AAGCTATCGCTGTACTTCCGGCA | GGCGTTGGCGCTCAGATAGG | |
| *rmpA* | 58 | ACTGGGCTACCTCTGCTTCA | CTTGCATGAGCCATCTTTCA | Yu et al., 2006 |
| *magA* | 52 | GGTGCTCTTTACATCATTGC | GCAATGGCCATTTGCGTTAG | |
| *wabG* | 52 | ACCATCGGCCATTTGATAGA | CGGACTGGCAGATCCATATC | |
| *K5* | 50 | TGGTAGTGATGCTCGCGA | CCTGAACCCACCCCAATC | Turton et al., 2008 |
| *fimH* | 58 | TGCTGCTGGGCTGGTCGATG | GGGAGGGTGACGGTGACAT | Yu et al., 2008 |
| *fyuA* | 58 | GCGACGGGAAGCGATGATTTA | TAAATGCCAGGTCAGGTCACT | Schubert et al., 2000 |

### 2.3 *Categorization of K.pneumoniae Isolates According to Their Virulence Profile*

The isolates who harbored at least two of the hypervirulence genes (*rmpA, iutA, peg344*) according to virulence gene screening were characterized as hypervirulence gene *Klebsiella pneumoniae* (hgKp). (Du et al., 2022)

### 2.4 *Hypervirulent Phenotype Assays for HgKp Isolates*

hgKp isolates were further analyzed for their hypervirulent phenotypes by string test and *C.elegans* fertility assay. (Du et al., 2022)

#### 2.4.1 *String Test for HgKp Strains*

All isolates were inoculated on 5% sheep blood agar and incubated overnight at 37℃. Then, colonies were picked with a loop and allowed for a sting to be formed. The strings formed >5mm were classified as string-positive isolates. (Fang et al., 2004)

### 2.4.2 *C.elegans Fertility Test*

Forty-eight hours *Caenorhabditis elegans* fertility test was performed for *in vivo* virulence analysis. (Sánchez-Diener et al., 2017) hgKp isolates were taken for *C.elegans* fertility assays. *C.elegans* npr-1 was seeded to 25 µL of nematode growth medium (NGM) containing OP50 *E.coli* strain and grown for about 2 days. Then, nematodes were collected when the nematodes reached the egg-laying phase and washed twice with 1M M9 buffer. Adult nematodes were pelleted and bleached with a lysis buffer containing 1% sodium hypochlorite and 62.5% sodium hydroxide. The mixture was shaken for 6 minutes at room temperature and washed twice with 1M M9 buffer. Bleached nematodes were incubated in 1.5 mL of M9 buffer at 25℃ overnight where they were exposed to light until the nematodes reached the L1 phase. During incubation, nematodes were checked under the Stereomicroscope. The next day, M9 buffer containing bleached nematodes was poured into 25 µL of nematode growth medium plate containing OP50 *E.coli* strain and incubated at 25℃ for 3 days until they reached the L4 growth phase. Five adult nematodes were picked and placed onto each well of the 6-well plates containing 100 µL of 0.5 McFarland bacterial suspension spread onto 2,5 µL of nematode growth medium. Viability, mobility, and fertility of nematodes were recorded in 24 and 48 hours. This experiment was done in duplicate. OP50 *E.coli* strain was used as a positive control for nematode growth. The virulence scores were decided according to the virulence scoreboard in Table 2.2. (Sánchez-Diener et al., 2017)

Table 2.2: *C.elegans* Virulence scores (CEV) according to the growth, proliferation inhibition, and nematode survival.

| *C.elegans* Virulence Score | | | |
|---|---|---|---|
| CEV1 | nematode n>50 | Inhibition of growth | Low |
| CEV2 | nematode n=5-50 | | |
| CEV3 | nematode n=5 | Inhibition of proliferation | Intermediate |
| CEV4 | nematode n=1-4 | Killing nematodes | High |
| CEV5 | nematode n=0 | | |

### 2.5 *Categorization of the Hypervirulent K. pneumoniae Isolates*

The hgKp strains who have exhibited a positive string test result (>5 mm) or a high virulence score in 48-hours *C.elegans* fertility assay according to virulence score board in Table 2.2. (Sánchez-Diener et al., 2017)

### 2.6 *Molecular Analysis of HvKp Isolates*

#### 2.6.1 *Multiple Locus Sequence Typing by Sanger Sequencing*

Seven housekeeping genes of *K.pneumoniae* (*rpoB, tonB, pgi, mdh, infB, phoE, gapA*) were amplified with conventional PCR according to the protocol on Institut Pasteur website (https://bigsdb.pasteur.fr/klebsiella/). (Diancourt et al., 2005) 12.5 µL of DreamTaq Green PCR master mix (Thermo Fisher Scientific, US) was supplemented with 0.5 µL of 25 pmol forward primer, 0.5 µL 25 pmol reverse primer, 5.5 µL betaine, and 5.5 µL nuclease-free water. For only the *tonB* reaction mixture 0.2 µL of $MgCl_2$ was used with 5.3 µL of nuclease-free water. Primer sequences and annealing temperatures were listed in Table 2.3. The reactions were performed with the following conditions; initial denaturation at 95°C, 2 min., 35 cycles of denaturation at 95°C, 35 sec., annealing at the corresponding melting temperature stated in Table 2.3, 35 sec., extension at 72°C, 45 sec. and final extension at 72°C, 5 min. 5 µL of PCR products were run in 1.5% agarose gel for 30 minutes at 90V. 5 µL of 1 kB GeneRuler ladder (Thermo Fisher Scientific, US) was run together with the PCR products.

PCR products were purified with NucleoSpin Gel and PCR Clean-up kit (Macherey-Nagel, Germany). 30 µL of nuclease-free water was added to 20 µL PCR product, and the solution was mixed with 100 µl of NT1 buffer. 150 µl solution was placed in a filtered collection tube and centrifuged at 11,000 g for 30 seconds. Flow-through was discarded. 700 µL of NT3 buffer was added onto the filter, and centrifuged at 11,000 g for 30 seconds. Flow-through was discarded. The filtered collection tubes were centrifuged for 1 minute at 11,000 g. The filters were placed on a new collection tube, and 20 µL of NE buffer was added to the filter. The filters were incubated at room temperature for 1 minute.

Collection tubes were centrifuged for 30 seconds at 11.000 g. Purified housekeeping gene samples were stocked in -20℃.

The purified PCR products were amplified with BigDye Terminator v3.1 Cycle (Applied Biosystems, U.S.). 1 µL of purified housekeeping sample was mixed with 2 µL BigDye, 1 µL of BigDye buffer, 3.2 µL of 1 pmol reverse primer, and 3.8 µL of nuclease-free water. The following conditions were used to amplify products: 1 min. at 96°C followed by 25 cycles of 10 sec. at 96°C, 5 sec. at 50°C, and finally 4 min. at 60°C. The PCR products were purified with ZR-96 DNA Sequencing Clean-up Kit (Zymo Research, U.S.) 20 µL of PCR product was mixed with 240 µl of binding buffer and the mixture was placed onto a filtered 96-well plate. The plate was centrifuged at 2576 rpm for 3 minutes. The flow-through was discarded. 300 µl of wash buffer was added onto the filtered 96-well plate and centrifuged at 2576 rpm for 7 minutes. The flow-through was discarded again. The filter was placed onto a clean 96-well plate and 20 µL of elution buffer was eluted via centrifugation at 2576 rpm for 3 minutes. The 96-well plate was loaded to Applied Biosystems ABI 3500 Genetic Analyzer, and the sequences of the housekeeping genes were obtained. Allelic profiles were created and sequence types were identified using Applied Math Bionumerics V7.6 software.

Table 2.3: Sequences and melting temperatures of MLST housekeeping primers.

| Name of the gene | $T_M$ (℃) | Sequence of Forward Primer | Sequence of Reverse Primer | Source |
|---|---|---|---|---|
| *rpoB* | 50 | GGCGAAATGGCWGAGAACCA | GAGTCTTCGAAGTTGTAACC | Diancourt et al., 2005 |
| *infB* | 55 | CTCGCTGCTGGACTATATTCG | CGCTTTCAGCTCAAGAACTTC | |
| *mdh* | 55 | CCCAACTCGCTTCAGGTTCAG | CCGTTTTTCCCCAGCAGCAG | |
| *pgi* | 55 | GAGAAAAACCTGCCTGTACTGCTGGC | CGCGCCACGCTTTATAGCGGTTAAT | |
| *tonB* | 52 | CTTTATACCTCGGTACATCAGGTT | ATTCGCCGGCTGGCRGAGAG | |

| | | | | |
|---|---|---|---|---|
| *phoe* | 60 | ACCTACCGCAACACCG ACTTCTTCGG | TGATCAGAACTGG TAGGTGAT | Diancourt et al., 2005 |
| *gapA* | 60 | TGAAATATGACTC CACTCACGG | CTTCAGAAGCGGCTTT GATGGCTT | |

### 2.7 *Plasmid and Amplicon Preparation*

#### 2.7.1 *Plasmid Confirmation by Restriction Digestion*

pMJH46 was a gift from Mark Liles (Addgene plasmid # 67272; http://n2t.net/addgene:67272 ; RRID:Addgene_67272, Addgene, US), stabbed in *E.coli*. (Hossain et al., 2015) Plasmid confirmation was done by restriction digest according to the manufacturer's instructions. (Addgene, 2018) *E.coli* was grown on 25 µL of LB agar 100 ug/mL ampicillin, 25 ug/mL chloramphenicol, and 0.1% L-arabinose. The plate was grown overnight at 30℃. Next day, a loop of colonies was passaged to 5 mL LB containing 100 ug/mL ampicillin, 25 ug/mL chloramphenicol, and 0.1% L-arabinose. The bacterial suspension was shaken overnight at 30℃ at 135 rpm. Total plasmid extraction was done with the NucleoSpin Plasmid kit (Macherey-Nagel, Germany). Fresh bacterial suspensions were pelleted by centrifugation for 30 seconds at 11,000 g. The pellets were suspended in 500 µL of Lysis Buffer A1 containing RNAse. After mixing properly, 500 µL of SDS/alkaline lysis buffer A2 was added to the solutions. The tubes were inverted 8 times and waited until a clear blue lysate appeared. Then, 600 uL of neutralization A3 buffer was added and the tubes were inverted until the blue solution becomes white completely. The lysates were cleared by centrifugation for 10 minutes at 11,000 g. The supernatants were loaded onto filtered tubes, and centrifuged for 1 minute at 11,000g. The flow-throughs were discarded and 500 µL of pre-heated Wash AW buffer was added to the filter. The filtered tubes were centrifuged for 1 minute at 11,000g. The tubes were again centrifuged at 11,000 g for 1 minute after the addition of 600 µL of Wash A4 Buffer. The silica membranes were dried by centrifugation at 11,000 g for 2 minutes. The filters were loaded to new collection tubes and 50 µL of pre-heated Elution AE buffer was added onto the silica membrane. The plasmid samples were eluted, and stored in -20℃.

10 µL of isolated pMJH46 plasmid were incubated together first with 1 µL of BsaI-HF restriction enzyme (New England Biolabs, US). 5 µL of 1X rCutSmart buffer (New England Biolabs, US) and 34 µL of nuclease-free water were mixed with the plasmid and restriction enzyme mixes. Secondly, 10 µL of isolated pMJH46 plasmid were incubated together with 1 µL of BsaI-HF and 1 µL of SpeI-HF restriction enzymes (New England Biolabs, US). 5 µL of 1X rCutSmart buffer (New England Biolabs, US) and 33 µL of nuclease-free water were mixed with the plasmid and restriction enzyme mixes. The mixtures were vortexed thoroughly and incubated at 37℃ for 1 hour. Unrestricted plasmid and restricted products were separated on 1.5% agarose gel for 30 minutes at 90V. pMJH46 plasmid was confirmed according to the lengths of restricted products. 1 kb Ladder (Thermo Fisher Scientific, US) was used for band length confirmation.

### 2.7.2 *Amplicon Confirmation by Sanger Sequencing*

The disrupted *peg344* (Δ*peg344*) amplicon containing *peg344* flanking regions of 211 to 351 and 738 to 834 base pairs surrounding a gentamicin acetyltransferase encoding gene (*GmR*) was designed (Macrogen, Inc., South Korea) (Bulger et al., 2017). The lyophilized amplicon was diluted in 30 µL of nuclease-free water and was amplified using designed primers annealing upstream and downstream of the amplicon, listed in Table 2.4. 1 µL of the amplicon was mixed with 12.5 µL of DreamTaq Green PCR master mix (Thermo Fisher Scientific, US), 0.5 µL of 25 pmol forward primer, 0.5 µL of 25 mol reverse primer, 10.5 µL of nuclease-free water. The polymerase chain reaction was performed with the following conditions; 95℃ for 2 minutes, 35 cycles of denaturation at 95℃ for 35 seconds, primer annealing at 59 ℃ for 35 seconds, elongation at 72℃ for 45 seconds, and final elongation at 72℃ for 5 minutes. 5 µL of the PCR product was run in 1.5% agarose gel at 90V for 30 minutes.

The rest of the PCR product, 20 µL, was purified using the NucleoSpin Gel and PCR Clean-up kit (Macherey-Nagel, Germany). 20 µL of PCR product was mixed with 30 µL of nuclease-free water, and 100 µL of NTI binding buffer. The mixture was added onto a filtered collection tube, and centrifuged at 11,000 g for 30 seconds. The flow-through was discarded, and 300 µL of NT2 wash buffer was added to the filter. The filtered tube was centrifuged at 11,000 g for 30 seconds. The filter was placed onto a new collection tube, and 20 µL of AE elution buffer was added to the silica membrane. The filter and elution

buffer were incubated at room temperature for 1 minute. The collection tube together with the filter was centrifuged at 11,000 g for 30 seconds. The purified amplicon was stored at -20℃.

Purified PCR product was amplified with BigDye Terminator v3.1 Cycle (Applied Biosystems, U.S.). 1 µL of the purified amplicon was mixed with 2 µL of BigDye, 1 µL of BigDye, 3,2 µL of 1 pmol reverse primer, and 12,8 µL of nuclease-free water. The following conditions were used to amplify the purified amplicon: 1 min. at 96°C followed by 25 cycles of 10 sec. at 96°C, 5 sec. at 50°C, and finally 4 min. at 60°C. The PCR product was purified with ZR-96 DNA Sequencing Clean-up Kit (Zymo Research, U.S.). 20 µL of PCR product was mixed with 240 µL of binding buffer, and placed into a filtered collection tube. The collection tube was centrifuged at 2576 rpm for 3 minutes. The flow-through was discarded. 300 µL of wash buffer was added to the filter, and the tube was centrifuged at 2576 rpm for 7 minutes. The flow-through was discarded, and the filter was placed onto a new collection tube. 20 µL of elution buffer was added onto the filter, and centrifuged at 2576 rpm for 3 minutes. The elution was loaded, and the sequence of the amplicon was obtained by Applied Biosystems ABI 3500 Genetic Analyzer. The obtained sequence of the amplicon was compared with the designed amplicon via NCBI Blast Tool (https://blast.ncbi.nlm.nih.gov/Blast.cgi?BLAST_SPEC=blast2seq&LINK_LOC=align2seq&PAGE_TYPE=BlastSearch).

Table 2.4: Sequences and melting temperature of primers for designed amplicon for disrupted-*peg344* gene.

| **Name of the gene** | **$T_M$ (℃)** | **Sequence of Forward Primer** | **Sequence of Reverse Primer** |
|---|---|---|---|
| Δ*peg344* gene | 59 | GGCCAGCGTCTATTTCAACTT | CAATGACGAGGGGGATAATC |

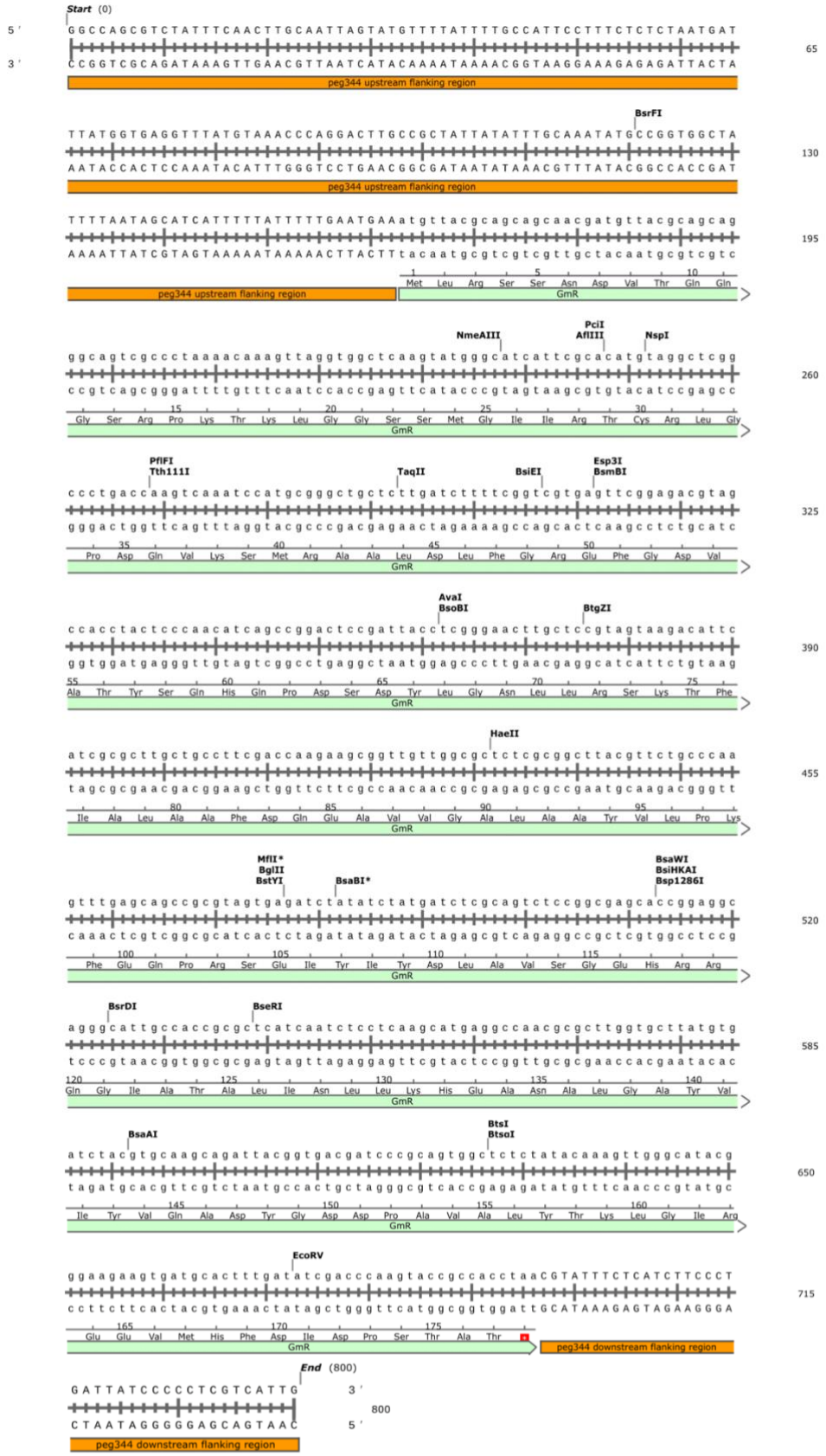


Figure 2.1: The sequence of the designed amplicon for *peg344* disruption containing *peg344* flanking regions of 211 to 351 and 738 to 834 surrounding a gentamicin acetyltransferase encoding gene (*GmR*).

### 2.8 *Capsule Inhibition Optimization by Negative Staining*

Capsule inhibition is suggested in order to increase the transformation efficiency of the encapsulated *K.pneumoniae* isolate. (Bulger et al., 2017) One loop of fresh culture was adjusted to 0.5 McFarland value in LB growth medium. 100 µL of bacterial suspension was added into 5 mL of LB containing 0.125 mM bismuth nitrate pentahydrate and 2.5 mM sodium salicylate (Merck & Co. Inc, US), and shaken overnight at 135 rpm in 37℃. The same *K.pneumoniae* sample was grown overnight in LB medium without any inhibitors for negative control. The next day, 10 µL of bacterial suspension was mixed with 10 µL Indian ink. 10 µL of stained bacteria were spread on a microscope slide and waited for 2 hours until the samples dried. The slides were fixed with heat fixation and counterstained with safranin for 30 seconds. The capsule formations were observed under the light microscope with 40x magnification. (Moyes et al., 2009)

One bacterial suspension with the McFarland value 0.5 was grown overnight in LB medium in order to compare the growth with the suspension grown in LB supplemented with capsule inhibitors. The OD value of both suspensions was measured. Also, both suspensions were diluted a hundredfold and 100 µL of each suspension were spread to TSA plates.

### 2.9 *peg344 Gene Disruption*

The Δ*peg344*-mutant was constructed using the **λ**red recombination method. (Bulger et al., 2017) HvKp isolate PF59 was inoculated on 25 µL of TSA and grown overnight in 37℃. The next day, one loop of colonies was passaged to 5 mL LB containing 0.125 mM bismuth nitrate pentahydrate and 2.5 mM sodium salicylate (Merck & Co. Inc, US), and shaken overnight at 135 rpm in 37℃. Overnight shaken bacterial cells were placed on ice for 20 minutes, and centrifuged at 4,000 rpm for 10 minutes at 4℃. The supernatant was discarded and the pellet was dissolved in 20 mL of 0.1 M ice-cold $CaCl_2$. The bacterial suspension containing 0.1 mM $CaCl_2$ was incubated in 4℃ for 30 minutes, and centrifuged for 10 minutes at 4,000 rpm at 4℃. The supernatant was discarded and the pellet was dissolved in 5 mL of 0.1 M $CaCl_2$ with 10% glycerol. Competent cells were stocked in -80℃. (Chang et al., 2017)

For heat-shock transformation, 50 µL of competent cells were thawed on ice, and mixed with 1 µL of PMJH46 plasmid. (Chang et al., 2017) Competent cell-plasmid mixture was incubated at 4℃ for 30 minutes. The mixture was incubated at 42℃ for exactly 30 seconds, and placed on ice for 2 minutes. Pre-warmed 1 mL of LB containing 0.1% L-arabinose (Merck & Co. Inc, US) was immediately added to the mixture and outgrown at 37℃ for 2 hours at 200 rpm. Outgrown bacteria were diluted tenfold, and 100 µL of diluted bacteria was spread on 25 µL LB agar plate containing 100 ug/mL ampicillin, 25 ug/mL chloramphenicol, and 0.1% L-arabinose. The selection plate was grown overnight at 30℃. Next day, colonies are picked, dissolved in %20 glycerol containing tryptic soy broth, and stored at -80℃.

One colony was passaged to 5 µL of LB containing 100 ug/mL of ampicillin, 25 ug/mL of chloramphenicol, 0.1% L-arabinose, 0,125 mM bismuth nitrate pentahydrate, 2,5 mM sodium salicylate (Merck & Co. Inc, US). The bacterial suspension was shaken overnight at 135 rpm at 37℃. Fresh LB culture was incubated on ice for 20 minutes, and pelleted by centrifugation at 4,000 g for 20 minutes at 4℃. The bacterial pellet was dissolved in 500 µL of ice-cold %10 glycerol. The bacterial suspension was centrifuged at 4,000 g for 20 minutes at 4℃. The pellet again dissolved in 500 µL of ice-cold 10% glycerol, and centrifuged at 4,000 g for 20 minutes at 4℃. The pellet is dissolved in 50 µL of ice-cold 10% glycerol. 40 µL of electrocompetent cells were mixed with 1 µL of designed amplicon. The electrocompetent cell-amplicon mixture was loaded onto a pre-chilled 0.1 mm cuvette and incubated on ice for 3 minutes. The cuvette is placed in MicroPulser electroporator (BioRad Laboratories, US), and a single pulse of 1.8 kV was applied. 1 mL of pre-warmed LB medium containing 0.1% L-arabinose was immediately added to the cuvette, and outgrown at 200 rpm 37℃ for 2 hours. The bacterial suspension was diluted tenfold and hundredfold, and 100 µL of each dilution was spread to a LB agar plate containing 10 ug/mL gentamicin, and 0.1% L-arabinose, and to a tryptic soy agar plate.

The non-selective TSA plate was grown overnight at 37℃. Gentamicin serial dilution MIC determination was performed in order to confirm the gentamicin resistance of the mutant strain. (Datsenko et al, 2000) Bacteria were dissolved in cation-adjusted Mueller Hinton broth and adjusted to a MacFarland value of 0.5. 256 ug/mL of gentamicin was serially diluted in 100 µL of Cation-adjusted Mueller Hunton broth containing a 96-well

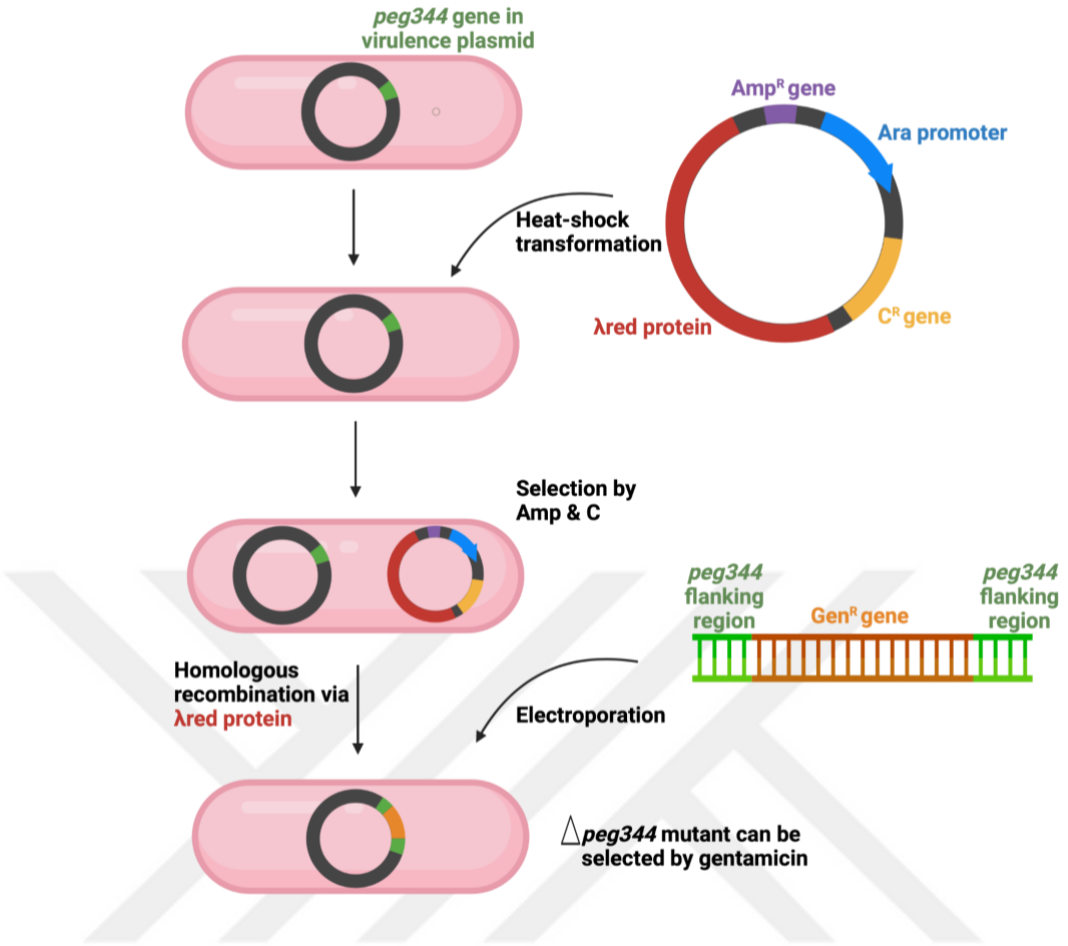


Figure 2.2: Schematic illustration of **λ**red recombination method for *peg344* gene disruption. Firstly, **λ**red recombinase encoding plasmid carrying ampicillin and chloramphenicol resistance genes, and L-arabinose promoter was introduced to the bacterium with heat-shock transformation. The bacteria transformed the plasmid was grown in the presence of L-arabinose, and selected via ampicillin and chloramphenicol. Secondly, the designed amplicon for *peg344* gene disruption was introduced to the bacteria via electroporation. The bacteria in which the homologous recombination was achieved accurately was grown in the presence of L-arabinose, selected by gentamicin.

U-bottom plate. 10 µL of bacterial suspension was added into each well except the 12th column in order to have a positive control well of bacterial growth.

The selective LB agar plate was incubated at 37℃ for 48 hours. Colonies grown on the selective plate were passaged to 3 mL of LB, and shaken overnight at 135 rpm at 37℃. 1 mL of bacterial suspension was passaged to 9 mL of LB, and shaken for 24 hours at 135 rpm at 37℃. One colony was mixed with 1.5 mL of TSB containing 20% glycerol in a cryo vial, stored in -80℃.

### 2.9.1 *Sequence Confirmation of the Δpeg344-pf59 Mutant*

Total plasmid of Δ*peg344*-PF59 strain was extracted using NucleoSpin Plasmid kit (Merck & Co. Inc, US) with the protocol written in section 2.6.1. 0.5 µL of isolated plasmid solution was mixed with 12.5 µL of 2x DreamTaq Green PCR Master Mix (Thermo Fisher Scientific, US), 11 µL of nuclease-free water, and 0.5 µL of forward and reverse primers written in Table 2.4. For the PCR, the following reaction conditions were used; initial denaturation at 94°C, 5 min., 30 cycles of denaturation at 94°C, 25 sec., annealing at 59°C, 40 sec., extension at 72°C, 50 sec. and final extension at 72°C, 6 min. 5 µL of the total PCR product were loaded onto 1,5% agarose gel, and the gel was runned for 40 minutes at 90V. 1 kb Ladder (Thermo Fisher Scientific, US) was loaded onto the gel for band length confirmation. The remaining 20 µL of PCR product was purified with NucleoSpin Gel and PCR Clean-up kit (Macherey-Nagel, Germany). The purified Δ*peg344* gene was amplified with BigDye Terminator v3.1 Cycle (Applied Biosystems, U.S.) The amplified product was purified with ZR-96 DNA Sequencing Clean-up Kit (Zymo Research, US). All of these protocols and conditions were explained in Chapter 2.6.1. The sequence of the disrupted peg gene was detected via Applied Biosystems ABI 3500 Genetic Analyzer. The sequence of the Δ*peg344* gene was compared with the designed amplicon using NCBI Blast Tool (https://blast.ncbi.nlm.nih.gov/Blast.cgi?BLAST_SPEC=blast2seq&LINK_LOC=align2seq&PAGE_TYPE=BlastSearch).

## 2.10 *Macrophage Infection*

### 2.10.1 *Macrophage Cell Differentiation from THP-1 Monocyte Cells*

Monocyte cells were stimulated to differentiate into macrophage cells according to the previous protocol. (Phuong et al., 2021) THP-1 monocyte cells TIB-202™ (ATCC®, US) were grown in 10% fetal bovine serum (FBS), 1% penicillin-streptomycin, and 1% L-glutamine containing RPMI 1640 medium. 4 x $10^6$ cells were inoculated to 6-well plates, and 100 nM of phorbol 12-myristate 13-acetate (PMA) was added to each well in the cell culture environment and avoided light exposure. The cells were incubated at 37℃ for 3 days in the incubator containing 5% $CO_2$. After incubation, the cells were washed with

PBS in order to eliminate PMA from the environment. The cells were again incubated in the incubator with 5% $CO_2$ for 24 hours in a complete medium.

For macrophage differentiation confirmation via flow cytometer, the cells that have been inoculated to the 6-well plate were harvested from the plate with 2 mL of accutase. The cells were incubated for 15 minutes 37℃ in the incubator with 5% $CO_2$. The cells were washed by centrifugation (400 g, 5 min, 4°C) with 1X PBS. The cells were stained in V-bottom 96-well plates with up to 3x 10^6 cells per well. For investigation of macrophage viability, cells were stained with 1:500 diluted in 1X PBS Zombie-NIR dye (BioLegend, USA). The cells were incubated in the dark for 15 minutes, and the cells were pelleted at 400 g for 5 minutes at 4°C. 50 µL of FACS buffer per well of the master mix was prepared containing pre-titrated amounts of the antibodies containing CD14, and CD68 surface markers plus 5 µl/mL of α-CD16/32-Ab (clone 2.4G2) (Beckton, Dickinson and Company, US). The master mix was added to the cells, resuspended, and incubated for 15-30 minutes on ice in the dark. After incubation, the cells were centrifuged and the pellet was washed twice with 150 µl PBS (400 g, 5 min, 4°C). The cells were run with Cytoflex SRT Flow Cytometer. (Phuong et al., 2021)

### 2.10.2 *Macrophage Phagocytosis Assay*

*In vitro* macrophage infection assay was generated with a previous protocol with slight modifications. (Phuong et al., 2021) One colony of fresh bacterial culture inoculated on 25 mL of TSA was passaged to 5 mL of LB medium, and shaken overnight at 135 rpm at 37℃ until they reached the logarithmic growth phase. Only the Δ*peg344*-mutant was grown in 5 mL of tryptic soy broth. 0.5 McFarland value was adjusted using 5 mL LB fresh culture and PBS. 1 mL of 0.5 McFarland bacterial suspension was pelleted by centrifugation at 20,000 g for 10 minutes. The supernatant was discarded, and the pellet is dissolved in 1 mL of human serum, 1:1 diluted with PBS. The bacteria-containing serum was incubated at 37℃ for 30 minutes. The eppendorf tube was incubated on ice for 2 minutes in order to stop the opsonization process. The bacteria were again centrifuged for 10 minutes at 20,000 g.

After opsonization and centrifugation of the opsonized bacteria, the pellet was dissolved in 500 µL of RPMI. 100 µL of bacterial suspension was added onto 2 mL of 600,000

macrophage cells in 6-well plates in order to obtain an infection assay with 1:50 moi. For the control of bacterial growth, 100 µL of diluted bacterial suspension was added onto 2 mL of RPMI, and incubated for 3 hours at 37℃. The bacteria-macrophage mixture was centrifuged at 2500 rpm for 7 minutes in order to fasten the encounter of bacteria to macrophage cells. The bacteria-macrophage mixture was incubated at 37℃ for up to 6 hours in a 5% $CO_2$ incubator and allowed the macrophage cells to phagocytose the opsonized bacteria.

### 2.10.3 *Bacterial Survival Assay upon Phagocytosis Assay*

100 uL of the bacteria-macrophage mixture and 100 µL of only bacteria-containing suspensions were serially diluted up to $10^{-7}$ at 0, 1, and 2, 3, and 6 hours after the beginning of infection. The serial dilutions of $10^{-3}$, $10^{-4}$, $10^{-5}$, $10^{-6}$, and $10^{-7}$ were inoculated onto duplicate plates of 25 mL of TSA, and grown overnight at 37℃. The colonies were counted after 18 hours, and the inhibition of bacterial growth was calculated compared to the control.

### 2.10.4 *Macrophage Viability and M1 & M2 Convergence Rate Analysis by Flow Cytometry*

600,000 THP-1 monocytes were seeded in 6-well plates with 2 mL of cell culture medium per well. The PMA stimulation was done as written in section 2.10.1. Before the infection assay, the cells were aspirated and a complete cell culture medium without antibiotics was added to the cells. The infection was simulated as written in section 2.10.2.

After 1 hour, 2 hours, 3 hours, and 6 hours of infection; 500 µL of accutase was added to wells and incubated for 7 minutes at 37℃ in a 5% CO2 incubator. The cells were collected from the plates and washed twice with 1X PBS. The cells were pelleted by centrifugation at 2,000 rpm for 5 minutes. The cells were resuspended in 700 µL of ice-cold 1X PBS, and 1 µL of viability dye Zombie NIR-APC-Cy7 was added in the cell suspension in a flow tube. The cells were incubated at dark for 10 minutes at 4℃. The cells were again pelleted by centrifugation at 2,000 rpm for 5 minutes, and resuspended in 1 mL of FACS buffer. Antibody mixture containing 1 µL of Cd11b-FITC, Cd86-BV650, Cd206-PECy5 (BioLegend, USA). was added to each suspension. The cells were incubated at dark for

15 minutes at 4℃. The cells were again pelleted at 2,000 rpm for 5 minutes and resuspended in 500 µL of PBS. Stained cells were run in Cytoflex SRT Flow Cytometer. The analyses were done with Flow.Jo software 7.1. The single cells were gated by forward scatter. Within single cells, live cells were identified using Zombie-NIR dye. From live single cells, CD11b expressing cells were categorized as macrophages. CD86 (M1 marker), and CD209 (M2 marker) expressing cell ratios were measured. Hence, macrophage viability, and M1 and M2 convergence rates after infection were obtained. (Andreata et al., 2021)

### 2.10.5 *Proinflammatory cytokine response analysis after the infection assay*

In order to measure the secreted cytokine level after the infection assay; the supernatants of 6 hours infection samples were collected from the 6 well plates. IL-1β, and TNFα cytokines' secretion will be measured with the ELISA kits for human IL-1β (DY201), and TNFα (DY210) (R&D Systems, US). The tests were done according to the manufacturer's instructions. The samples were tested in duplicates. (Phuong et al., 2021)

# CHAPTER 3

# RESULTS

## 3.1 *Characteristics of the K.pneumoniae Cohort*

Table 3.1: Number of isolates according to their isolation years and sources.

| Isolation Year | Number of isolates | Region |
|---|---|---|
| **2015-2016** | 116 | Ankara, Istanbul |
| **2017- 2018** | 86 | Istanbul |
| **2019-2021** | 14 | Istanbul |
| **2022-2023** | 14 | Ankara, Denizli, Istanbul |

Two-hundred-thirty *K.pneumoniae* strains isolated between January 2015 and March 2023 were included in the study. In the study population, 155 isolates were carbapenem-resistant, whereas 151 isolates were colistin-resistant. 143 isolates were resistant to both carbapenem and colistin.

### 3.1.1 *Molecular Characteristics of the Cohort*

MLST analysis revealed 23 different sequences respectively; ST101 (35%, 81/230), ST395 (7%, 16/230), ST999 (4%, 9/230), ST16 (3%, 7/230), ST2096 (3%, 6/230), ST147 (2%, 4/230), ST45 (2%, 4/230), ST23 (1%, 3/230), ST649 (>1%, 2/230), ST39 (>1%, 2/230), ST37 (>1%, 2/230), ST11 (>1%, 2/230), ST280 (>1%, 2/230), ST607 (>1%, 2/230), ST4838 (>1%, 1/230), ST29 (>1%, 1/230), ST86 (>1%, 1/230), ST5 (>1%, 1/230), ST307 (>1%, 1/230), ST609 (>1%, 1/230), ST54 (>1%, 1/230), ST888 (>1%, 1/230), ST192 (>13%, 1/230), ST268 (>1%, 1/230), non-assigned (34%, 78/230).

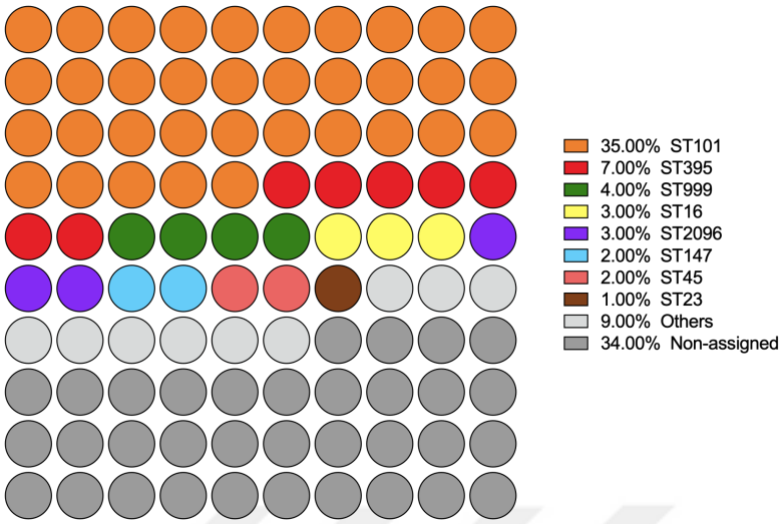


Figure 3.1: The percentages of sequence types in the *K.pneumoniae* cohort (n=230).

All samples were screened for 13 virulence genes (*peg344, iutA, rmpA, wabG, fyuA, kfu, ybtS, entB, mrkD, fimH, allS, magA, K2, K5*) via conventional PCR. The prevalence of each virulence gene among the cohort was indicated in Figure 3.1.

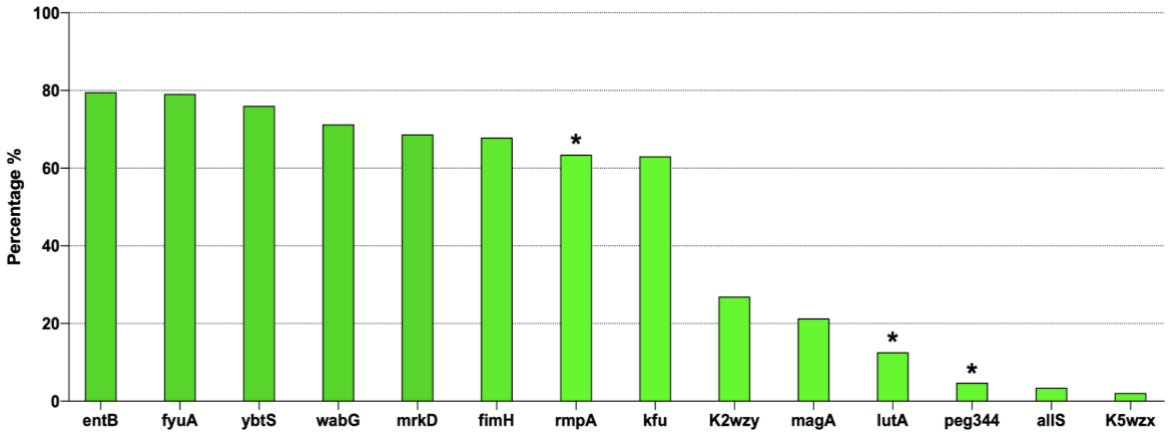


Figure 3.2: The percentages of 13 virulence genes among the *K.pneumoniae* isolates (n=230). The hypervirulence genes *rmpA, peg344,* and *iutA* were marked with an asterisk (*).

## 3.2 *peg344 Gene Disruption*

### 3.2.1 *Capsule Inhibition Optimization by Negative Staining*

OD value of the suspension grown overnight in LB medium was measured as 0.539, whereas the OD value of the suspension of the same isolate grown overnight in LB supplemented with 0.125 mM bismuth nitrate pentahydrate and 2.5 mM sodium salicylate was measured as 0.277.

According to the colonies spread on TSA plates, the colony count of the bacteria grown in LB medium was calculated as 18 x$10^{10}$ cfu/mL. The colony count of the bacteria grown in LB supplemented with 0.125 mM bismuth nitrate pentahydrate and 2.5 mM sodium salicylate was calculated as 14 x $10^{10}$ cfu/mL.

Hence, the addition of 0.125 mM bismuth nitrate pentahydrate and 2.5 mM sodium salicylate to the LB medium was optimized with the conditions that the chemicals inhibit the capsule expression but do not inhibit the growth of the bacteria.

**A** **B**

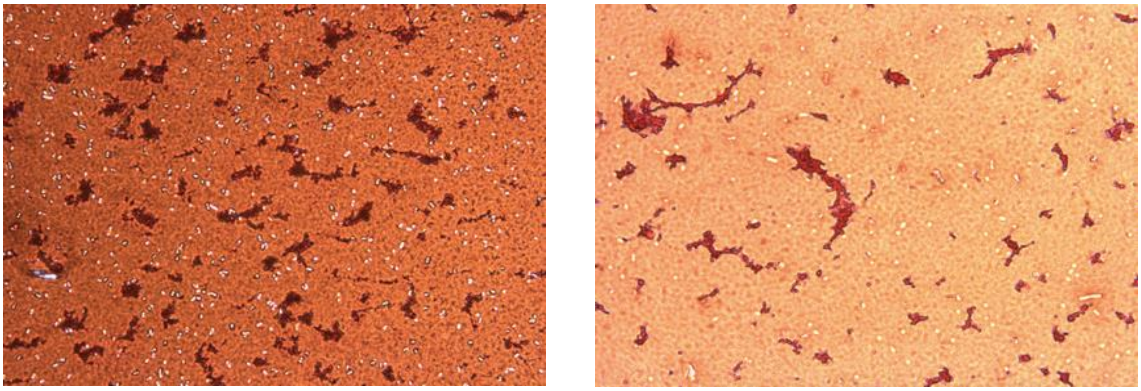

Figure 3.3: Light microscope images of negative stained bacteria under 40x magnification. A. The bacteria were grown overnight in LB and negatively stained. B. Image after negative staining of the same isolate that was grown overnight in LB supplemented with 0.125 mM bismuth nitrate pentahydrate and 2.5 mM sodium salicylate. White hallows indicate the capsule proteins. A decrease in the number of white hallows depending on the addition of capsule inhibitors was seen.

### 3.2.2 *Confirmation of Lambda red plasmid by Restriction Digestion*

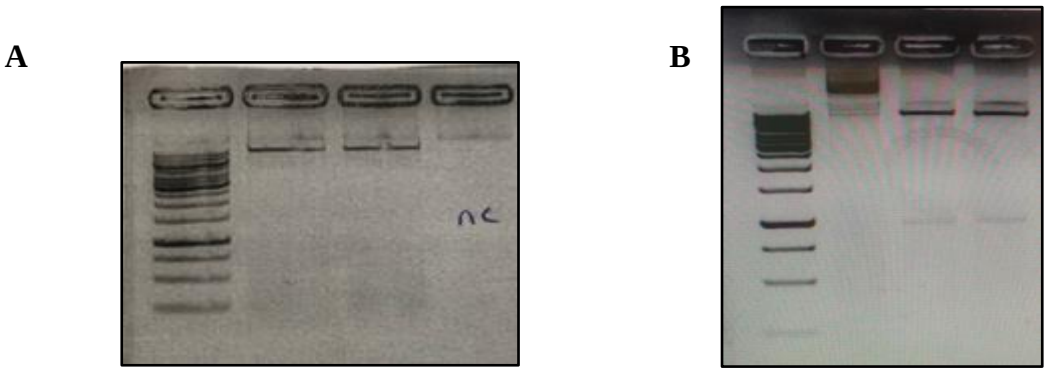


Figure 3.4: Agarose gel images of restricted plasmid together with 1 kB ladder. A. The plasmid was restricted with the BsaI-HF restriction enzyme. The band at 9661 bp indicated linear DNA after the single restriction. The last well was loaded with negative control for PCR. B. The plasmid was restricted with BsaI-HF and SpeI- HF restriction enzymes. Two bands were observed at 959 bp, and 8,702 bp after double restriction. The first well contains the unrestricted plasmid.

pMJH46 #67272 plasmid was restricted with 1 µL of BsaI-HF restriction enzyme, and also a combination of 1 µL of BsaI-HF, and 1 µL of Spe1-HF restriction enzymes. The restricted products were separated on 1.5% agarose gel. The gel images can be seen in Figure 3.4. The expected band length, 9661 base pairs, was observed in the gel with the product that has been restricted with only the BsaI-HF enzyme. In the gel containing the plasmid that has been restricted with BsaI-HF, and Spe1-HF restriction enzyme, two different bands with the lengths 959 bp, and 8,702 bp were observed. The uncut plasmid was observed with a higher length because of its circular conformation.

### 3.2.3 *Confirmation of the Designed Disrupted-peg344 Gene Amplicon by Sanger Sequencing*

The sequence of the disrupted *peg344* gene carrying amplicon was obtained via Sanger sequencing, and the sequence was aligned with the sequence of the designed amplicon using NCBI Blast Tool (https://blast.ncbi.nlm.nih.gov/Blast.cgi). The sequence of the disrupted *peg344* amplicon was confirmed by Sanger sequencing as seen in Figure 3.5.

**A**

| Max Score | Total Score | Query Cover | E value | Per. Ident | Acc. Len | Accession |
|---|---|---|---|---|---|---|
| 1367 | 1367 | 100% | 0.0 | 100.00% | 800 | Query_125421 |

**B**

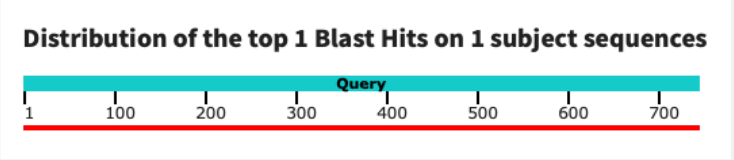


Figure 3.5: NCBI Blast images for sequence confirmation for the designed amplicon. A. The alignment score of the sequenced amplicon and the sequence of the design. 100.00% alignment was observed. B. Query of the alignment of the sequenced amplicon and the sequence of the design.

### 3.2.4 *Confirmation of the Constructed Δpeg344-PF59 Mutant by Sanger Sequencing*

After allowing the recombination of the disrupted *peg344* gene harboring amplicon within the bacterial plasmid, the *peg344* gene of Δ*peg344*-PF59 mutant was amplified.

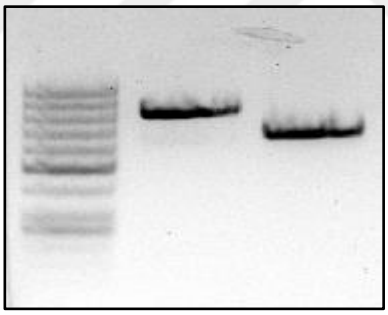

Figure 3.6: Agarose gel image of disrupted *peg344* gene together with wild-type *peg344* gene after λred recombination. The disrupted peg344 gene was observed as 147 base pairs longer than the wild-type *peg344* gene. 50 kB Ladder was loaded to the first well.

The PCR product containing the disrupted *peg344* gene was run together with the wild-type *peg344* gene on an agarose gel. Compared to the 1 kB ladder (Thermo Fisher Scientific, US); the disrupted p*eg344* gene was observed as 800 base pair long, whereas wild-type *peg344* was observed as shorter, 653 base pair long, as expected. The homologous recombination of the amplicon into the virulence plasmid was confirmed via PCR amplification and agarose gel separation.

The sequence of the gene was obtained via Sanger sequencing. The sequence of the *peg344* gene of the Δ*peg344*-PF59 mutant was aligned with the sequence of the designed amplicon. The sequence of the disrupted *peg344* gene within the mutant strain was confirmed via Sanger sequencing. Hence, the homologous recombination of the amplicon containing the *peg344* flanking region and gentamicin resistance gene into the *peg344* gene was confirmed via Sanger sequencing.

**A**

| Max Score | Total Score | Query Cover | E value | Per. Ident | Acc. Len | Accession |
|---|---|---|---|---|---|---|
| 1397 | 1423 | 96% | 0.0 | 100.00% | 774 | Query_23921 |

**B**

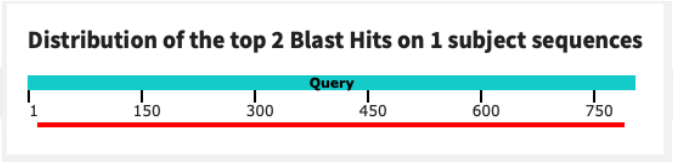


Figure 3.7: NCBI Blast images for sequence confirmation for the *peg344* gene disruption. A. The alignment score of the sequenced amplicon and the sequence of the amplified *peg344* gene. 100.00% alignment was observed. B. Query of the alignment of the sequenced amplicon and the sequence of the amplified *peg344* gene.

### 3.3 *Phenotypic Differentiation of Hypervirulence Gene Harboring Isolates*

hgKp isolates together with Δ*peg344*-PF59 mutant were further analyzed with string and *C.elegans* lethality test for their hypervirulent phenotypes. (Du et al., 2022)

#### 3.3.1 *String Test Results*

Fourteen out of twenty-two isolates have exhibited hypermucoviscous colonies and a string >5 mm was formed during string test on 5% sheep blood agar. Hence, 59% of the hgKp isolates have exhibited hypermucoviscous phenotype.

As expected, wild-type PF59 and Δ*peg344*-PF59 exhibited similar results in the string test, both isolates were found to be string-positive. This result confirms reexpression of capsule proteins after the capsule inhibitors bismuth nitrate pentahydrate, and sodium salicylate were eliminated from the growth medium. (Bulger et al., 2017)

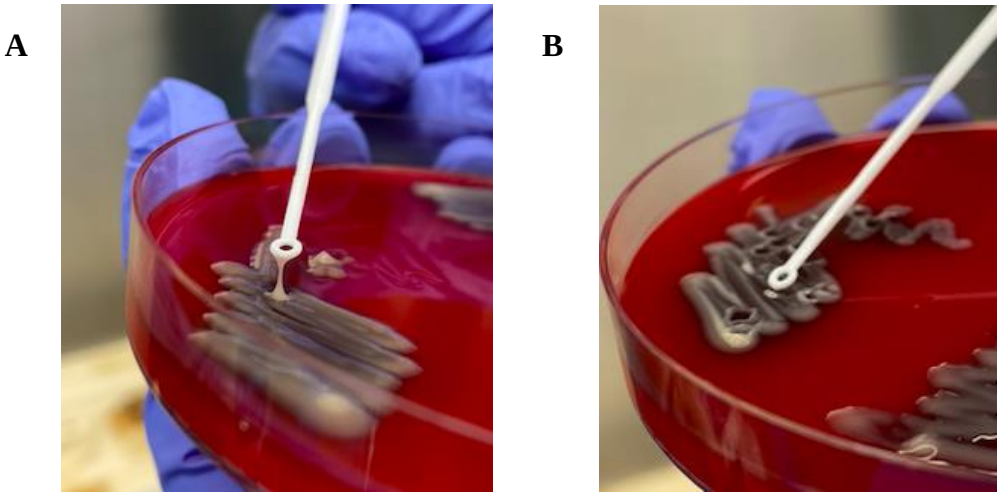


Figure 3.8: Images during the string test assays on hypervirulence gene harboring isolates. A. Image of a string test assay with a string formation >5 mm, positive for string formation. B. Image of a string test assay without a string formation, negative result.

### 3.3.2 *C.elegans Fertility Test Results*

Forty-eight hours *C.elegans* fertility assay was performed with hgKp isolates and Δ*peg344*-PF59 mutant. The virulence scores were defined according to the virulence scoreboard in Table 2.2 (Sánchez-Diener et al., 2017). The isolates that have >3 CEV scores at 48 hours were defined as highly virulent in the *C.elegans* infection model.

The dispersion of CEV scores among overall variants tested (cKp n=10, hgKp n=8, hvKp n=13) was shown in Figure 3.9. The percentages of virulent phenotypes such as hypermucoviscosity and high virulence in the C.elegans model was shown in Figure 3.9. String test results were found to be significantly higher in hvKp strains compared to hgKp strains ($p=0.0032$). Also, hvKp strains were found to be significantly more lethal at 48 hours of *C.elegans* model than hgKp and cKp strains ($p<0.0001$). The high fatality in the 48 hours *C.elegans* model emphasizes the clinical importance of hvKp and the need for screening for the hypervirulent profile.

PF59 and Δ*peg344*-PF59 strains were compared in 24 and 48 hours of CEV score. CEV score of wild-type pf59 isolate was found 4 in 24 hours, and 3 in 48 hours. Meanwhile, the CEV score of Δ*peg344*-PF59 strain was found 2 in both 24 and 48 hours.

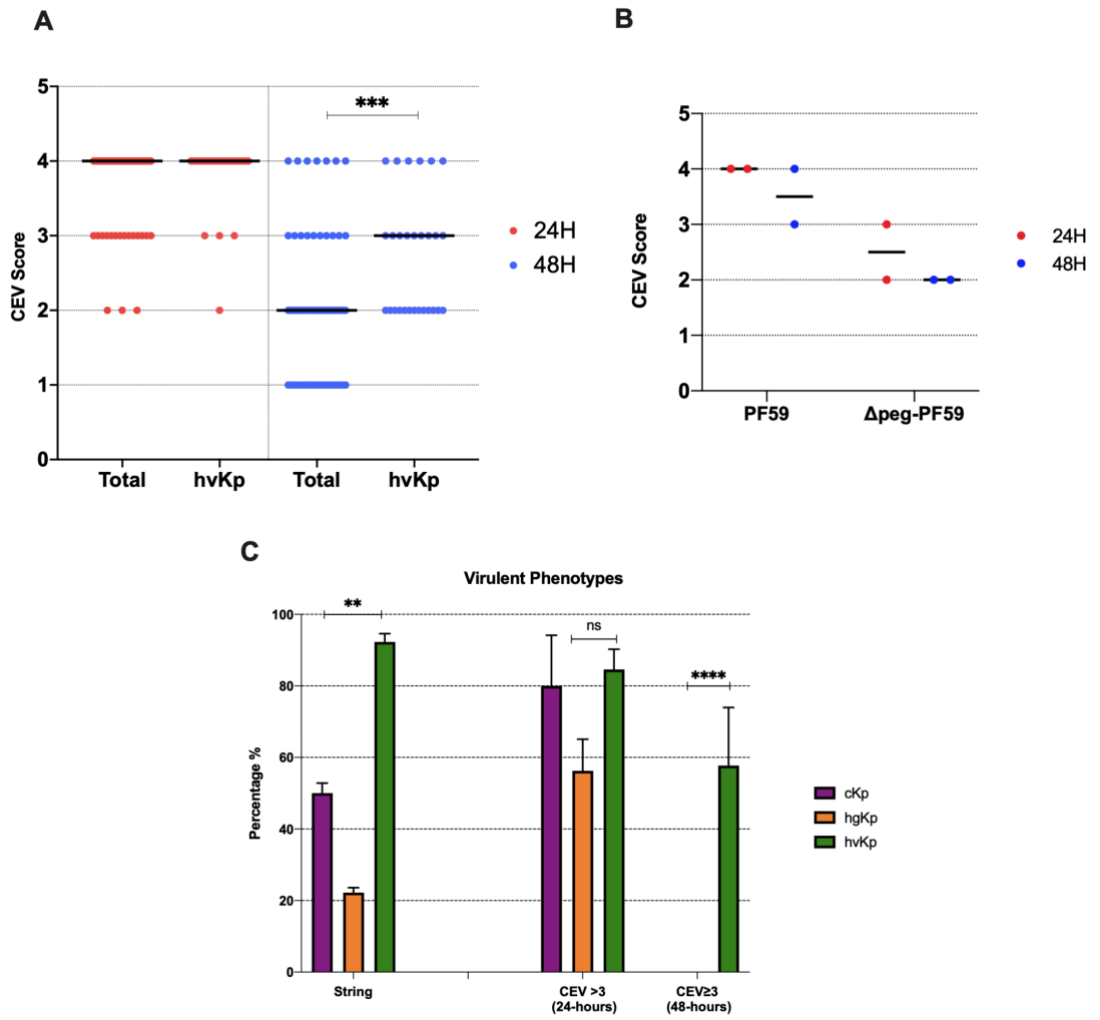


Figure 3.9: Results of phenotypic assay. A. The dispersion of CEV scores among all strains tested (n=31) and hypervirulent cohort including NTUH-K2044 (n=14). The median 48-hour CEV score of the hypervirulent cohort was significantly higher than the median 48-hour CEV score of all cohorts (p=0.007). B. Compared *C.elegans* virulence scores of PF59 and Δ*peg344*-PF59 isolates in 24-hours and 48-hours. C. String test results and *C.elegans* virulence score according to the variants (cKp n=10, hgKp n=8, hvKp n=13). Positive string test results of hvKp strains were significantly higher than hgKp strains (p=0.0032). 48-hour *C.elegans* virulence score of hvKp strains was significantly higher than hgKp and cKp strains (p<0.0001). 24-hour *C.elegans* virulence scores of hypervirulent strains were insufficient for differentiating between hgKp (0.0592) and cKp variants (p=0.7131).

### 3.4 *Differentiation and Characteristics of hvKp isolates*

hgKp isolates that have exhibited a positive string test or a high *C.elegans* virulence score (>3 at 48 hours) in 48 hours are categorized as hypervirulent *Klebsiella pneumoniae.* 13 (5.65%) isolates out of 22 hgKp strains were categorized as hvKp. Genotypic and phenotypic characteristics are indicated in Table 3.1. (Du et al., 2022)

Table 3.2: Genotypic and phenotypic characteristics of hypervirulence gene harboring isolates; hgKp and hvKp.

| Sample Codes | ST Types | Virulence Genes | Resistance to Carbapenem & Colistin | String Test | CEV score (48-hours) | Variant |
|---|---|---|---|---|---|---|
| **K1445** | 2096 | *peg344, wabG, fyuA, kfu, iutA,ybtS, entB, fimH, magA* | carbapenem | negative | 1 | hgKp |
| **CRK21** | 101 | *wabG, fyuA, kfu, iutA, ybtS, entB, mrkD, fimH, rmpA, K2wzy* | both | negative | 1 | hgKp |
| **CRK217** | 999 | *wabG, fyuA, kfu, iutA, ybtS, entB, mrkD, fimH, rmpA* | both | negative | 1 | hgKp |
| **CRK24** | 101 | *wabG, fyuA, kfu, iutA, ybtS, entB, fimH, rmpA* | both | negative | 1 | hgKp |
| **CRK40** | 101 | *wabG, fyuA, kfu, iutA, ybtS, entB, mrkD, fimH, rmpA* | both | negative | 2 | hgKp |
| **CRK49** | 649 | *wabG, fyuA, kfu, iutA, ybtS, entB, mrkD, fimH, rmpA, magA* | both | negative | 1 | hgKp |
| **CRK50** | 395 | *wabG, fyuA, kfu, iutA, ybtS, entB, mrkD, fimH, rmpA* | both | negative | 1 | hgKp |
| **GNB161** | novel | *iutA, entB, rmpA* | none | positive | 1 | hgKp |
| **K1317** | 2096 | *fyuA, kfu, iutA, ybtS, entB, mrkD, fimH, magA* | carbapenem | positive | 1 | hgKp |
| **K1315** | 2096 | *peg344, wabG, fyuA, kfu, iutA, ybtS, entB, mrkD, fimH, magA* | carbapenem | positive | 3 | hvKp |
| **K1341** | 2096 | *peg344, wabG, fyuA, kfu, iutA, ybtS, entB, mrkD, fimH, rmpA, magA* | carbapenem | positive | 3 | hvKp |
| **K1343** | 2096 | *peg344, wabG, fyuA, iutA, ybtS, entB, mrkD, fimH, magA, K2Wzy* | carbapenem | positive | 3 | hvKp |

| | | | | | | |
|---|---|---|---|---|---|---|
| **K1441** | 23 | *peg344, allS, wabG, fyuA, kfu, iutA, ybtS, entB, mrkD, fimH, rmpA, magA* | none | positive | 3 | hvKp |
| **CRK59** | 888 | *wabG, fyuA, kfu, iutA, ybtS, entB, mrkD, rmpA* | both | positive | 3 | hvKp |
| **GNB173** | 101 | *iutA, entB, rmpA* | carbapenem | positive | 2 | hvKp |
| **K1596** | 23 | *peg344, allS, wabG, fyuA, iutA, ybtS, entB, mrkD, fimH, rmpA, magA* | none | positive | 4 | hvKp |
| **K1915** | 23 | *peg344, allS, wabG, kfu, iutA, magA* | none | positive | 2 | hvKp |
| **PF59** | 86 | *peg344, wabG, fyuA, kfu, ybtS, entB, mrkD, fimH, rmpA, K2Wzy* | carbapenem | negative | 2 | hvKp |
| **TR131** | 307 | *peg344, allS, wabG, fyuA, kfu,ybtS, entB, mrkD, rmpA* | none | negative | 3 | hvKp |
| **K2025** | 268 | *peg344, wabG, fyuA, iutA, ybtS, entB, mrkD, fimH, rmpA* | both | positive | 2 | hvKp |
| **K1873** | 4838 | *wabG, kfu, iutA, entB, mrkD, fimH* | none | positive | 2 | hvKp |
| **TR133** | 2096 | *peg344, allS, wabG, kfu, iutA, entB, mrkD, rmpA, fimH* | both | positive | 4 | hvKp |

In the cKp cohort; 134 strains were resistant to carbapenem and colistin, 5 strains were carbapenem-resistant, 8 isolates were colistin-resistant, and 61 isolates were susceptible to both antimicrobials.

### 3.4.1 *Molecular Characteristics of HvKp Isolates*

#### *Prevalence of Hypervirulence Genes peg344, iutA, rmpA*

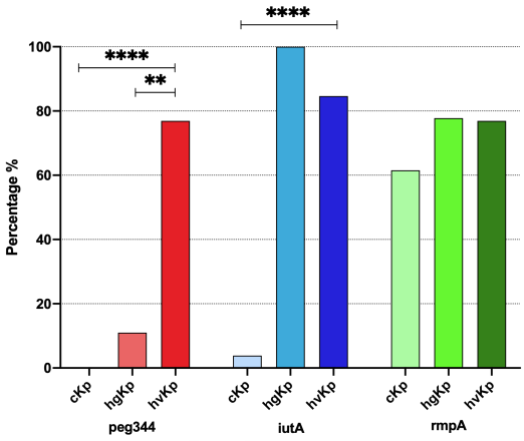


Figure 3.10: Prevalences of hypervirulence genes *peg344*, *iutA*, *rmpA* among 3 variants. *peg344* was significantly more prevalent in hvKp group compared to hgKp (p=0.0075) and cKp group (p<0.0001).

The hypervirulence gene prevalence among variants was visualized in Figure 3.10. Each of them was highly prevalent among hvKp strains; 76.92%, 84.62%, and 76.92% respectively. hvKp prevalence of the *peg344* gene was significantly higher than hgKp (p=0.0075) and cKp (p<0.0001) prevalence. Also, the prevalence of the *iutA* gene in hvKp was higher compared to cKp isolates (p<0.001). There was no significant difference in *rmpA* gene prevalence between cKp and hvKp (p=0.3806).

#### *Prevalence of Other Virulence Genes*

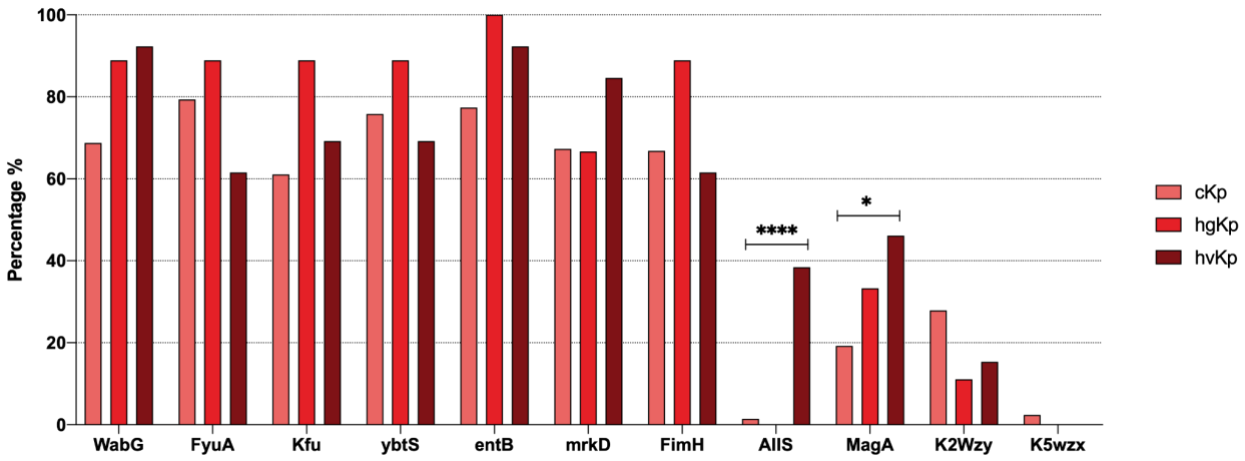


Figure 3.11: Prevalences of other virulence genes among variants. *allS* and *magA* were significantly more prevalent in hvkP group (p<0.0001, p=0.316 respectively.)

Ten different virulence genes (*wabG, fyuA, kfu, ybtS, entB, mrkD, fimH, allS, magA, K2, K5*) were screened for all isolates. The prevalence among variants were shown in Figure 3.11. Among all virulence genes, significantly higher prevalence in hvKp strains was observed in *allS* (38.46%, p<0.0001) and *magA* (46.15.%, p=0.316) genes compared to cKp strains (1.44%, 19.23%, respectively).

***Sequence Types of HvKp Isolates***

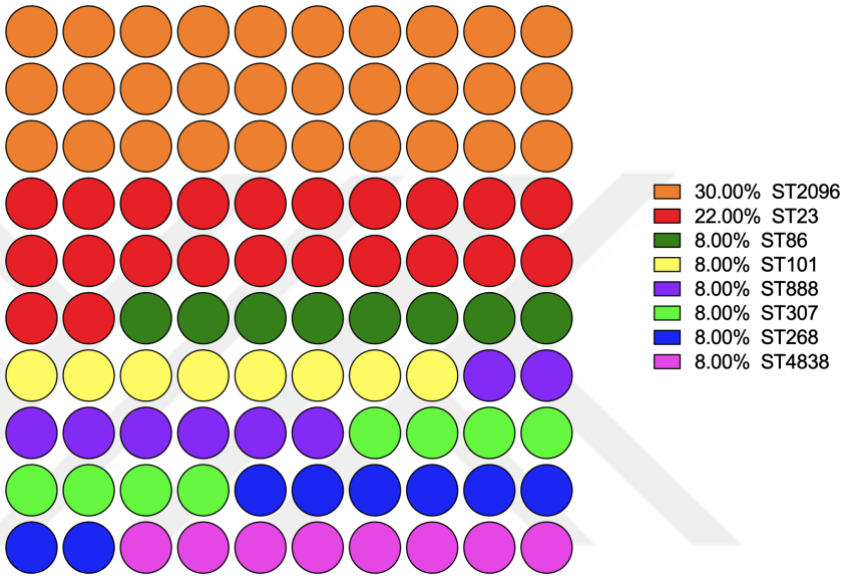


Figure 3.12: Percentages of STs of all hypervirulent strains.

MLST analysis revealed 8 different sequence types were identified (ST2096, ST23, ST86, ST101, ST888, ST307, ST268, ST4838) among 13 hypervirulent isolates. ST2096 was found as the most prominent clone in hypervirulent isolates (4/13, 30%), followed by the universal hypervirulent clone ST23 (3/13, 22%). ST86 (1/13, 8%), ST101 (1/13, 8%), ST888 (1/13, 8%), ST307 (1/13, 78%), and ST268 (1/13, 8%), ST4838 (1/13, 8%) clones were detected in the hvKp cohort.

***Capsular Serotypes of HvKp Isolates***

K1, K2, and K5 capsule serotypes were screened among 13 hypervirulent isolates via conventional PCR. Six isolates were found to express K1 capsular serotype (6/13, 46.15%) which was determined as the most prominent capsule type. Two of the isolates were found positive for K2 capsular serotype (2/13, 15.38%). None of the isolates were

found to express K5 capsular serotype. All of the ST23 isolates (3/3, 100%) were found to express K1 capsular serotype. Three isolates harbored ST23-K1 genotype among the hypervirulent cohort. (3/13, 22%) One hypervirulent isolate express the ST86-K2 genotype (1/13, 8%).

### 3.4.2 *Prevalence of hypervirulence according to Antimicrobial Resistance Profile*

Out of the 140 isolates which were co-resistant to carbapenem and colistin, 4 isolates were detected as hypervirulent (2.8%, 4/140). Among 12 isolates that were resistant to carbapenem but not colistin, 5 strains were categorized as hypervirulent (41.67%, 5/12). None of the eight isolates resistant to colistin only were identified as hypervirulent (0%, 0/8). Seven hypervirulent isolates were detected among the carbapenem and colistin-susceptible group (4/67, 5.97%).

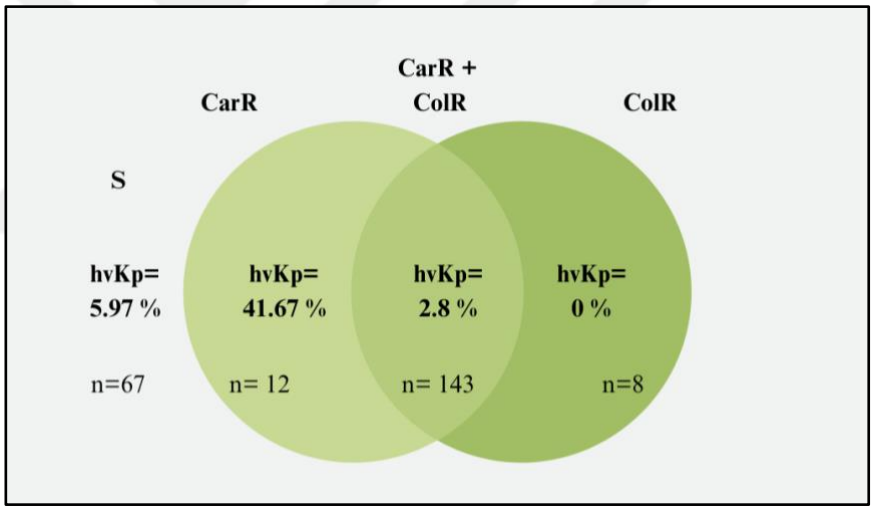


Figure 3.13: Prevalences of hypervirulent isolates according to their carbapenem and colistin resistance; co-resistant (n=143), carbapenem-resistant (n=12), colistin-resistant (n=8), susceptible (n=67) isolates.

### 3.4.3 *Timeline of hypervirulence prevalence*

The prevalence of hypervirulent *K.pneumoniae* according to the isolation years were indicated in Figure 3.14. Between 2015-2016, 1 isolate was found as hypervirulent (1/116, 0.86%). Among the isolates isolated between 2017-2018, 4 isolates were hypervirulent (4/86, 4.65%). 3 isolates were categorized as hypervirulent (3/14, 21.43%), whereas 5 isolates were found to be hypervirulent between 2022-2023 (5/13, 35.71%).

The hypervirulence prevalence between 2022-2023 was significantly higher than 2017-2018 (p=0.024), and 2015-2016 (p<0.0001). The increase of hypervirulence prevalence in 2022-2023 compared to 2019-2021 was non-significant (p=0.6776).

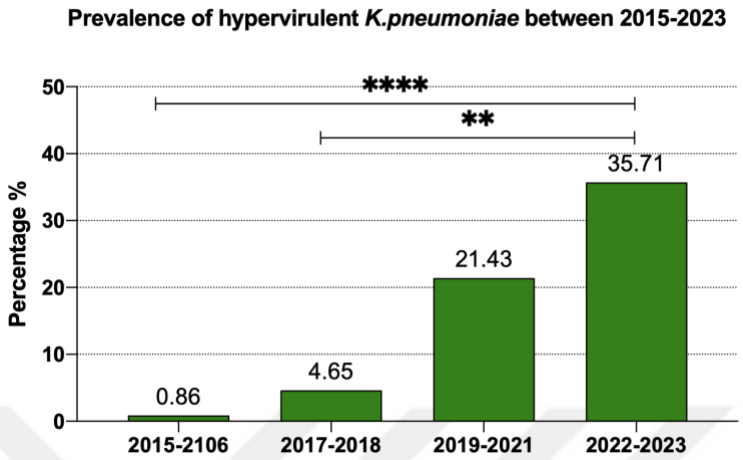


Figure 3.14: Percentages of hypervirulent strains according to the isolation years; 2015-2016 (n=116), 2017-2018 (n=86), 2019-2021 (n=14), 2022-2023 (n=14). The prevalence of hypervirulent strains between 2022-2023 was significantly higher compared to the prevalence between 2017-2018 (p=0.0024), and between 2015-2016 (p<0.0001).

## 3.5 *Macrophage Phagocytosis Assay*

### 3.5.1 *Confirmation of THP-1-driven Macrophage Cells by Flow Cytometry*

The unstimulated THP-1 monocytes and PMA stimulated cells were observed under a Leica light microscope with a 40X objective as seen in Figure 3.15. THP-1 monocytes were observed in suspension whereas the cells were observed as attached to the surface after 3 days of PMA stimulation. In order to confirm the macrophage cell differentiation from THP-1 cells, PMA-stimulated THP-1 cells were dyed with Zombie-NIR for viability and surface markers CD14 and CD68. The Zombie-NIR negative cells were gated as viable cells. The cells with low expression of CD14 (lower than $10^2$) and high expression of CD68 (higher than $10^2$) were categorized as macrophage cells. The macrophage differentiation percentage was found as 91.5%, shown in Figure 3.15. (Phuong et al., 2021)

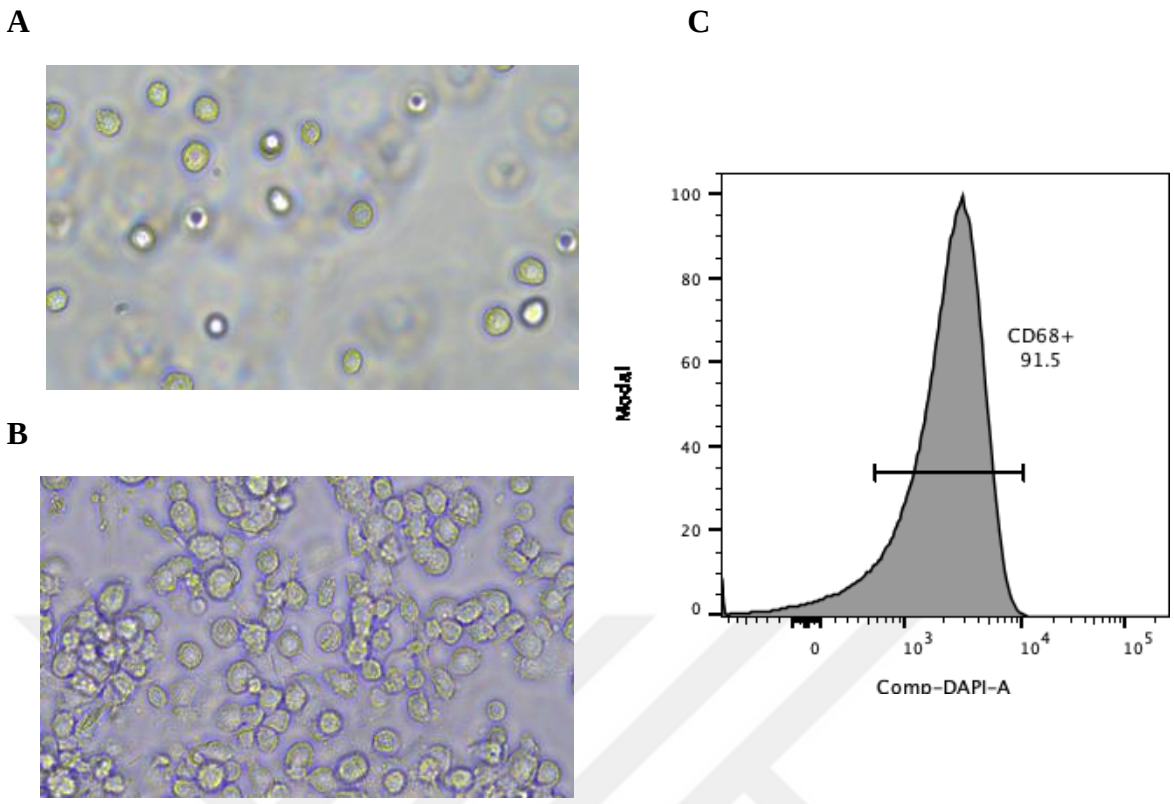


Figure 3.15: THP-1 driven macrophage cells confirmation results. A. Image of THP-1 monocyte cells under 40x magnification. B. Image of THP-1 cells under 40x magnification after 3 days of PMA stimulation. C. Flow.Jo analysis result. Cells expressing CD86 $>10^2$ and CD16 $>10^2$ were gated among the cells that were negative for Zombie-NIR dye.

### 3.5.2 *Bacterial Survival Analysis Upon Macrophage Phagocytosis Assay*

Macrophage cells were infected with ATCC strain 700831 (ATCC®, US), NTUH-K2044, cKp (n=3), hgKp (n=3), hvKp (n=3), PF59, and Δ*peg344*-PF59 samples. After 1, 2, 3, and 6 hours, the supernatant of the infected macrophages were taken, diluted, and spread to TSA plates. By comparing the colony count of bacterial growth samples, bacterial growth inhibition by macrophages was measured as indicated in Figure 3.16.

Macrophage cells were able to inhibit bacterial growth of cKp (3 clinical isolates and ATCC 700831) strains for each time point of infection with an inhibition percentage of >50%. For hgKp samples (3 clinical isolates), macrophage cells inhibited bacterial growth at 1 hour, and 2 hours (68.5%, and 78.5% respectively). However, at the 3-hour time point, the growth of hgKp samples was higher in the supernatant of macrophages

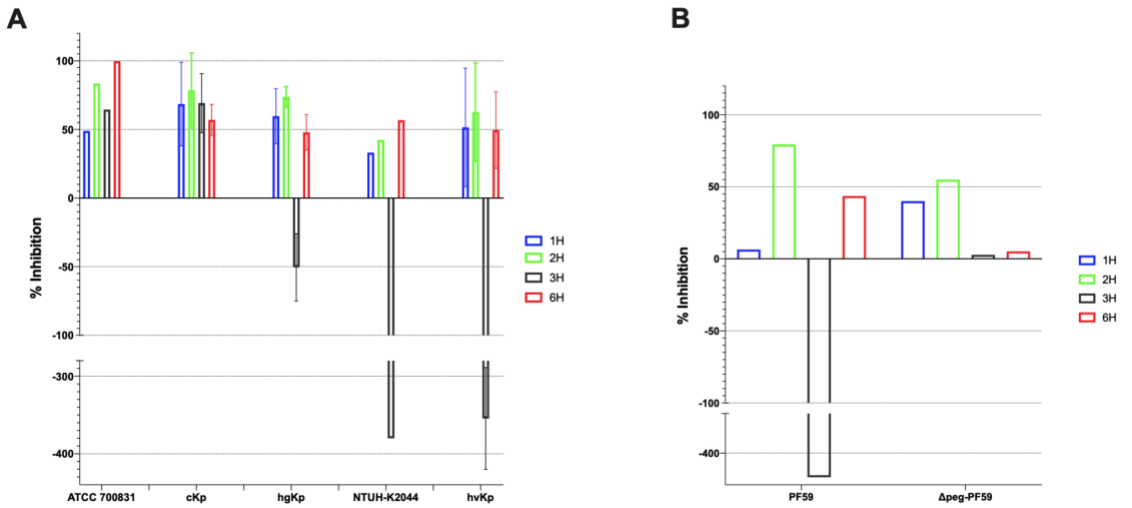


Figure 3.16: Bacterial growth inhibition percentages after macrophage phagocytosis assay. A. Total macrophage inhibition of bacterial growth according to variants ATCC 700831, cKp (n=3), hgKp (n=3), NTUH-K2044, hvKp (n=4). B. Compared growth inhibition of PF59 and Δ*peg344*-PF59 mutant after the macrophage infection assay.

compared to the control. The percentage of growth of hgKp samples were 50.5% at 3-hour infection. At 6-hour infection, macrophage cells have recovered the killing capacity by inhibiting bacterial growth by 48%. In the macrophages infected with hvKp samples (4 clinical samples and NTUH-K2044), macrophages inhibited the bacterial growth in 1, and 2 hours (51.5%, and 61.5% respectively). Similar to hgKp samples, hvKp isolates were able to outgrow at the 3-hour time point, the percentage growth was 355% compared to the control. However, macrophages have recovered their inhibition capacity to 50% at 6-hour time point, similar to hgKp samples. The inhibition percentages of hvKp isolates have shown the same tendency as the NTUH-K2044 strain as seen in Figure 3.16a.

The growth inhibitions of PF59 and Δ*peg344*-PF59 mutant upon macrophage phagocytosis assay were compared in Figure 3.16b. PF59 isolate showed a similar inhibition trend to hvKp samples as expected. However, Δ*peg344*-PF59 mutant showed a different trend in bacterial growth inhibition than PF59 isolate which was closer to cKp isolates at 3-hour of infection. At 3 hours of infection, macrophages inhibited the growth of Δ*peg344*-PF59 by 3%, whereas PF59 had grown 430% higher compared to the control.

### 3.5.3 *Macrophage Viability Analysis Upon Phagocytosis Assay*

After the infection; the macrophage cells were elevated, and stained with Zombie-NIR dye for 1, 2, 3, and 6 hours of infection. The viability of macrophages according to the variants were indicated in Figure 3.17a.

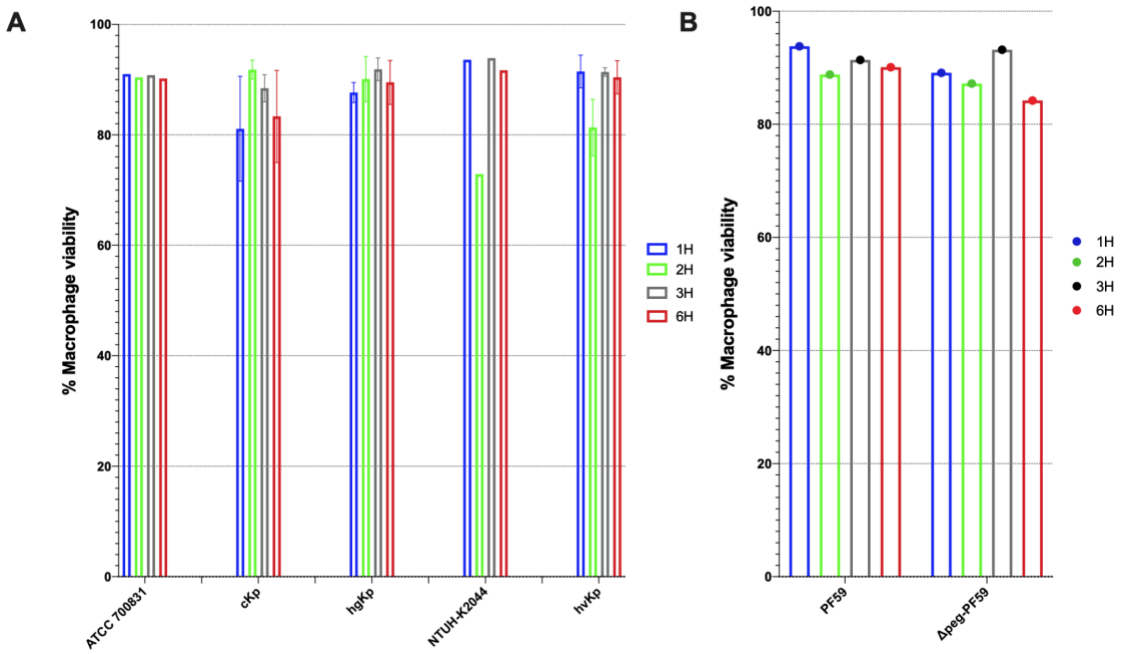


Figure 3.17: Viability of macrophage cells after infection. A. Macrophage viability according to different variants ATCC 700831, ckP (n=3), hgKp (n=3), NTUH-K2044 and hvKp (n=4). B. The compared macrophage viability for 4 time points of infection of PF59 and Δ*peg344*-PF59 mutant.

Macrophage cells infected with ATCC 700831 strain had high viability for every time point of infection, higher than 90%. Similarly, the macrophages infected with cKp isolates had similar viability results at 1, 2, 3, and 6 hours (>80%). For hgKp isolates, the macrophage viability at each time point was higher than 90%, similar to cKp ATCC 700831 strain. High viability was observed in the macrophage cells infected with NTUH-K2044 hypervirulent strain at 1-hour, 3-hour, and 6-hour time points. However, at the 2-hour time point, there was a drastic decrease in macrophage viability to 73%. The macrophages infected with hypervirulent isolates had the same tendency of macrophage viability similar to NTUH-K2044. A decrease in the viability of macrophages at 2-hour time point to 81.5%, together with high viability at other time points was observed. At

the 2-hour time point, the live macrophage cell ratio infected with hvKp was significantly lower than the live macrophage cell ratio infected with cKp isolates (p=0.0159).

The viability of macrophages infected with PF59 and Δ*peg344*-PF59 mutant were compared in Figure 3.17b. At each time point, the macrophage viability was higher than 80% for both isolates. A slight decrease in macrophage viability was observed in the 2 hours of infection at macrophages infected with PF59, from 93% to 89%. There was no decrease in the viability of macrophages infected with Δ*peg344*-PF59 at 2 hours of infection.

### 3.5.4 *M1 & M2 Convergence Rates upon Phagocytosis Assay*

CD86 expressing inflammatory and CD209 expressing anti-inflammatory macrophage cell ratios according to the variants and time points of infection was indicated in Figure 3.18.

CD86 expressing inflammatory M1 macrophage cells decreased from 18% to11.5% in the first 6 hours of infection when infected with hvKp isolates. On the contrary, when infected with cKp isolates, M1 macrophages tended to increase from 5% to 13% in the first 6 hours of infection. At 2 hours of infection when the viability macrophage cells was at the lowest level (Figure 3.17a), the M1 ratio was lower when infected with hvKp (10%) compared to cKp (17.6&) (ns, p=0.2857). At the 6 hours of infection, the M1 ratio of hvKp strains was sustained as lower than cKp (11.5%, and 14% respectively) strains, as seen in Figure 3.18a.

In contrast to M1 macrophages, CD209 expressing M2 macrophages were increasing during 6 hours of hvKp infection, from 18% to 27%. During the first 6 hours of cKp infection, the M2 macrophage cell ratio decreased from 25% to 19%. At the 2-hour time point, M2 ratio decreased in all variants, but the recovery of M2 macrophages at 6 hours was higher in hvKp infection. Hence, hvKp isolates evoked the anti-inflammatory response earlier than cKp, and anti-inflammatory responses were sustained at the 6-hour time point as indicated in Figure 3.18b.

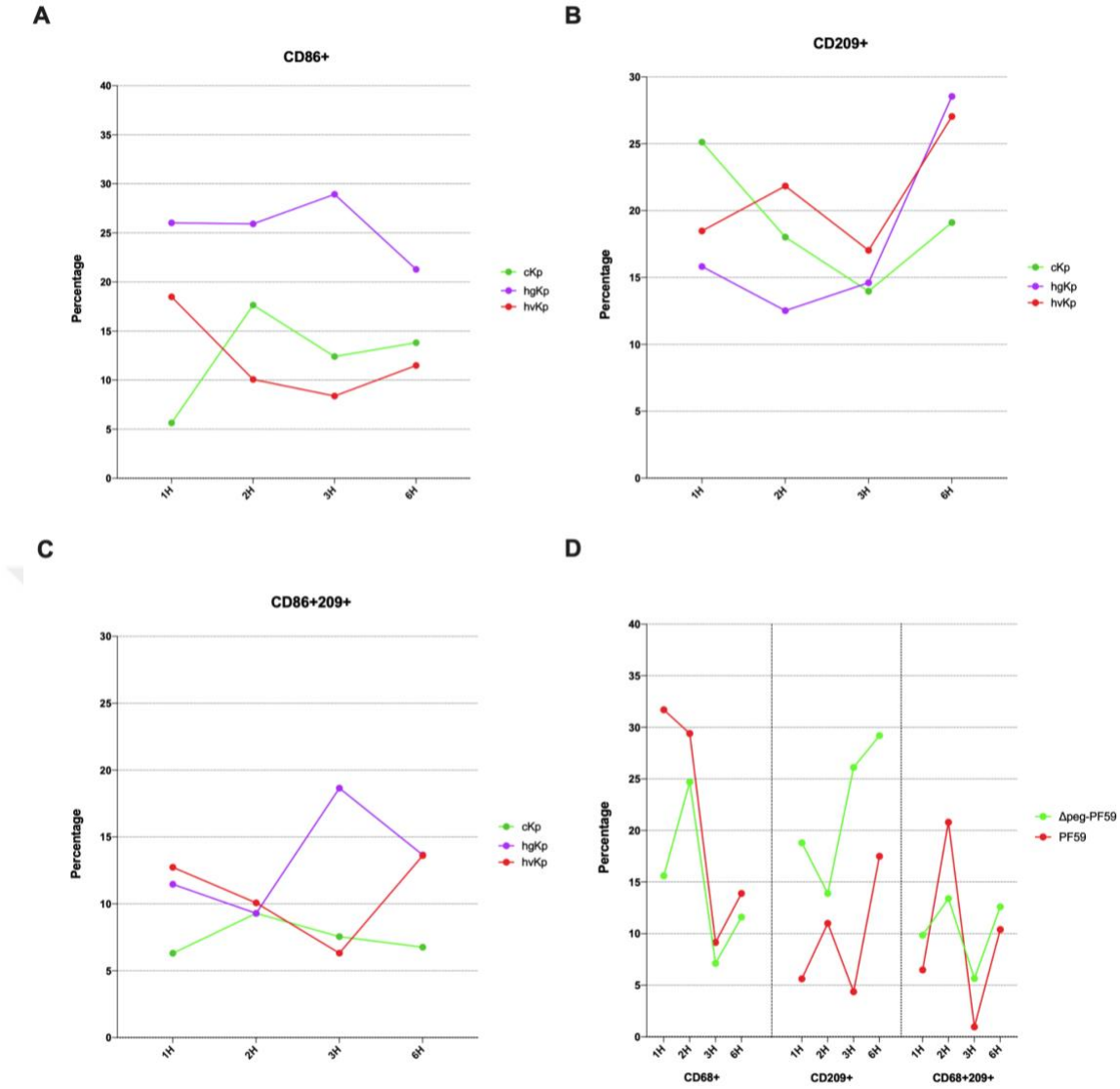


Figure 3.18: M1 and M2 marker expression percentages of different variants ckP (n=4), hgKp (n=3), and hvKp (n=5) for different time points. A. The percentages of CD68+ cells within variants for different infection time points. B. The percentages of CD209+ cells within variants for different infection time points. C. Ratios of C68+209+ cells within variants for different infection time points. D. Comparative percentages of CD68+, CD209+, and CD68+209+ macrophage cells infected with PF59 and Δ*peg344*-PF59 mutant at different time points of infection.

Similar trends in M1 and M2 convergence ratios during the first 6 hours of experiment was observed in both PF59 and Δ*peg344*-PF59 mutant infection which can be seen in Figure 3.18d.

### 3.5.5 *Cytokine Secretion Analysis upon Phagocytosis Model*

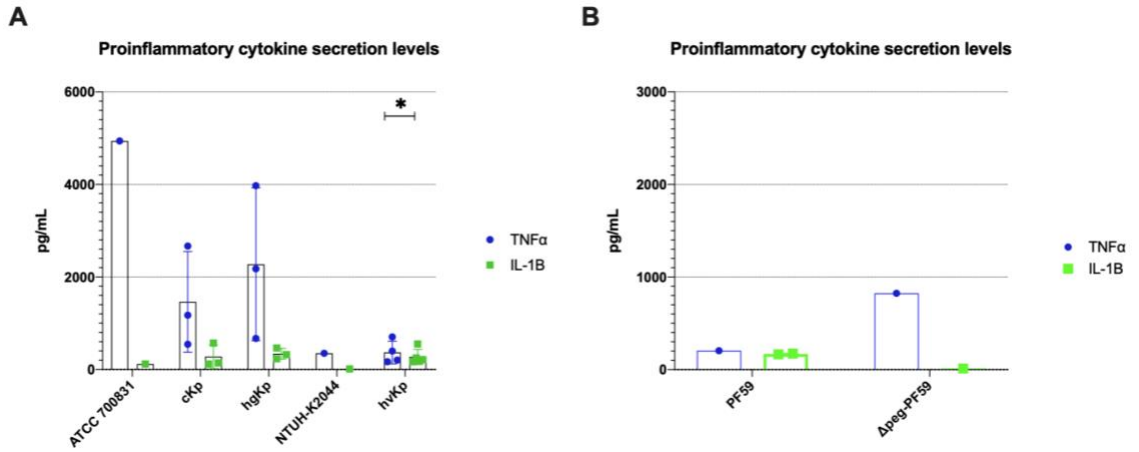


Figure 3.19: Cytokine secretion analysis. A. IL-1β and TNFα secretion analysis upon 6 hours of infection model according to the variants ATCC 70081, cKp (n=3), hgKp (n=3), NTUH-K2044, hvKp (n=4). TNFα secretion was significantly higher in macrophages infected with cKp compared to macrophages infected with hvKp (p=0.0159). B. Comparative cytokine secretion analysis of PF59 and Δ*peg344*-PF59 mutant at 6 hours of infection.

IL-1β and TNFα cytokine secretion amounts upon 6 hours of macrophage infection were compared with ELISA kits. The number of cytokines released per variant was indicated in Figure 3.19a. IL-1β release upon cKp, hgKp, and hvKp infection was observed in the low levels. Meanwhile, TNFα release upon hvKp infection was significantly lower than cKp infection (368, 1462 pg/mL respectively, p=0.0159)

The cytokine secretion amounts of macrophages infected with PF59 and Δ*peg344*-PF59 isolates were compared in Figure 3.19b. IL-1β secretion was observed in low levels in both isolates, whereas Δ*peg344*-PF59 infection had caused a higher amount of TNFα secretion compared to PF59 infection (203 vs. 824 pg/mL). The *peg344* deletion had recovered the proinflammatory cytokine, TNFα secretion levels of PF59, closer to cKp isolates (1462 pg/mL).

# Chapter 4

# DISCUSSION

The aim of this study was to determine the prevalence of hypervirulent *K.pneumoniae* in Turkey and to determine how the *peg344* gene modulates the innate immune response. Hypervirulent strains are emerging pathogens, currently, cases are being reported worldwide. (Hallal Ferreira Raro et al., 2023; Ombada et al., 2023; Zou et al.,2023) The initial strains were generally susceptible to many antimicrobials. (Wyres et al., 2020) However, in recent years they are converging to carbapenem-resistant hypervirulent strains which pose a serious global threat. (Chen et al., 2018; Tian et al., 2023) Before the prevalence of carbapenem-resistant hypervirulent *K.pneumoniae* (CarR-hvKp) increases drastically, the pathogenesis of hvKp should be elucidated in order to combat CarR-hvKP. In a study published in 2021, 10% of 111 isolates from Ankara were categorized as hvKp. (Örsten et al., 2020) In our study, 5.65% (13/230) of the samples were categorized as hvKp. Yet, there is not any study in Turkey focusing on the surveillance information hvKp or CarR-hvKp or the immune modulation role of the *peg344* gene in hvKp infections. There is an urgent need for studies concerning the evolutionary success of hypervirulent strains.

Even though the Asian Pacific Rim has reported more cases of hvKp infection than any other region, the cases are seen worldwide and the rates of hvKp infections are increasing by year. (Chung et al., 2007; Hsieh et al., 2008; Hallal Ferreira Raro et al., 2023; Ombada et al., 2023; Zou et al., 2023) The rate of carbapenem-susceptible-hvKp has increased from 0.4% to 27.03% between 1980-2022 in a study covering 105 countries. (Wu et al., 2022) In this study, a significant increase in hvKp infections was observed between the years 2015-2023. Among the strains from Istanbul, Ankara, and Denizli; hvKp incidence increased 41-fold from 2015 to 2023. The rapid emergence of Multidrug-resistant hypervirulent *K.pneumoniae* (MDR-hvKp) isolates highlights the importance of the pathogen in our region.

Identification of hypervirulent strains is still complicated, a consensus has not been reached yet on the criteria for hypervirulent differentiation in the literature. (Harada et al., 2018) Recently, Russo and his colleagues identified 5 biomarker genes (*peg344, iroB, iucA, rmpA, rmpA2*) that differentiate hypervirulent genes with high accuracy. (Russo et al., 2018). In our study, the *peg344* gene was significantly higher in hvKp compared to hgKp ($p=0.075$) and cKp isolates ($p<0.0001$). The aerobactin prevalence among *K.pneumoniae* strains is increasing in our region. Previously, the prevalence of *iutA* was determined 5.7% in 2017, and 7.2% in 2020. (Kuş et al.,2017; Örsten et al., 2020) In our cohort, even though the *iutA* gene was rare (3.85%) in cKp; the gene was highly prevalent in hgKp (100%) and hvKp (84.62%) isolates. Hence, the *iutA* gene may be a biomarker for differentiating hgKp and hvKp strains from cKp isolates ($p<0.0001$), but it is not a discriminative marker between hgKp and hvKp strains according to this study. The *rmpA* prevalence was observed as 0% in two studies and as 34% in a study from Turkey. (Candan et al., 2015; Kuş et al.,2017; Örsten et al., 2020) Just like *iutA, rmpA* prevalence is increasing in Turkey. In our study, the *rmpA* gene was highly prevalent in all *K.pneumoniae* isolates (63.48%). However, there was no significant difference in *rmpA* prevalence among variants ($p=0.3806$). Therefore, it is not a good biomarker for differentiating hypervirulent strains in Turkey.

Several articles suggested a combination of phenotypic validation together with genotypic assays for hypervirulent differentiation. (Shi et al., 2018; Russo et al., 2018; Du et al., 2022) The prevalence of hypermucoviscosity in the hvKp differs between 51% to 98%. (Fang et al., 2004; Lee et al., 2006; Yu et al., 2008; Catalán-Nájera et al., 2016) The hypervirulent cohort in this study contained 92.3% string-forming hypermucoviscous isolates. The prevalence of hypermucoviscosity is significantly higher than hgKp (22%, $p=0.032$), but not for cKp isolates (50%, $p=0.0515$). Even though the rate of positive string tests is relatively higher than in other studies, we concluded that it should not be considered as an indicator of hypervirulence, individually. Therefore, we conducted a *C.elegans* fertility assay. Having a 48-hour *C.elegans* virulence score higher than 3, was significantly more common in the hypervirulent cohort ($p<0.0001$) than the hgKp and hvKp isolates. Even though high lethality in the *Galleria mellonella* model was documented for hypervirulent strains, *in vivo C.elegans* model was not priorly documented. (Gu et al., 2018; Li et al., 2020). A combined phenotype validation of string

test results and 48-hour *C.elegans* virulence score confirmed the hypervirulence identification by genotypic screening.

To elucidate the pathogenesis mechanism of hypervirulent strains, we conducted *in vitro* macrophage phagocytosis assay. Hypervirulent isolates significantly decreased the viability of macrophages at 2 hours of infection. While decreasing the viability, hvKp isolates converted a lower ratio of inflammatory M1 macrophages (10%) and a higher ratio of anti-inflammatory M2 cells (22%), compared to cKp isolates (18.5%, and 18% respectively). By evoking an anti-inflammatory response in the early phases of the infection, hvKp isolates were capable to grow within the macrophages at the 3-hour time point. Moreover, at the 6-hour time point, hvKp isolated significantly inhibited the secretion of TNFα ($p=0.0159$), but there was no difference in IL-1β levels. The macrophage hypophagia is an important factor in the resistance to immune responses. (Pinney et al., 2020) To our knowledge, there is no study that demonstrated macrophage hypophagia with hvKp isolates. Our findings may support the evidence of immune evasion strategies for hvKp. The induction of macrophage hypophagia might serve to the increase in invasion of the infection. Hence, hypervirulent isolates evoke the anti-inflammatory response by macrophages in the early stages of infection and delay the inflammatory response by innate immune cells. Recently, it was found that the outer membrane vesicles secreted upon hvKp infections stimulate the IL-8 secretion by activating nuclear factor NF-κB. Even so, there was no significant difference in the IL-8 secretion between cKp and hvKp infections. (Li et al., 2023) Based on our findings, we postulated that hvKp suppress macrophage response in the early phases of the phagocytosis. Therefore, TLR expressions or caspase pathways should be analysed in detail.

The *peg344* is a putative gene that was detected in the complete genome and transcriptome analysis in 2017. The *peg344 gene* was found as an accurate biomarker for hypervirulence in several studies (Bulger et al., 2017; Russo et al., 2018; Shen et al., 2020). However, the function or pathogenesis mechanism of the gene was still not elucidated. There is not yet any functional analysis concerning the *peg344* gene. In 2017, Bulger and his colleagues confirmed that *peg344* deletion decreases the lethality of the bacteria in the mouse model. (Bulger et al., 2017) Similarly in our study, the deletion of the *peg344* gene decreased the *C.elegans* lethality in both 24 and 48 hours. However,

*peg344* deletion didn't affect the string test results, to our knowledge there was no finding on the effect of the *peg344* deletion gene on the string test results. Since the gene encodes a metabolite transporter on the inner membrane, *peg344* deletion did not affect hypermucoviscosity.

There is not yet any study focusing on the effect of the *peg344* gene on the virulence at cellular level as well. In this study, Δ*peg344*-mutant was used *in vitro* macrophage infection, and the immune responses were compared to the wild-type strain. The *peg344* deletion didn't affect the viability, M1, and M2 convergence ratio of macrophages. However, peg344 deletion affected bacterial inhibition and TNFα secretion level. Δ*peg344*-PF59 mutant was inhibited by macrophages by 3%, whereas wild-type PF59 isolate was able to grow by 430% within the macrophages at 3 hours of infection. In a study, hypervirulent isolates expressing K1 and K2 capsule serotypes are found to be more resistant to phagocytosis by immune cells. (Wanford et al., 2021). The resistance of PF59 to phagocytosis at 3 hours of infection can be explained by its K2 capsule serotype. Yet, *peg344* deletion made the bacteria more prone to phagocytosis. Also, the TNFα secretion level of Δ*peg344*-PF59 (824.3 pg/mL) was higher than PF59 (203.5 pg/mL). The strong part of our study is that the contribution of the *peg344* gene to hypervirulent pathogenesis at the cellular level was not priorly documented. In order to elucidate the hypervirulent pathogenesis, more studies should be focusing on the *peg344* pathogenesis.

Hypervirulent strains generally express K1 and K2 serotypes. (Zhu et al., 2021; Du et al., 2022) K1 and K2 type capsule proteins make the bacteria more resistant to phagocytosis and intracellular killing by immune cells. (Wanford et al., 2021) Our findings support the high prevalence of K1 (46.15%), and K2 (15.38%) capsule serotypes among hypervirulent strains. K1-ST23 and K2-ST86 genotypes are very common hypervirulent lineages. (Pei et al., 2023; Hallal Ferreira Raro et al., 2023) Twenty-two percent of our hypervirulent isolates have harbored the K1-ST23 genotype, whereas eight percent of the cohort harbored the K2-ST86 genotype. These results prove that K1-ST23 and K2-ST86 are global hypervirulent lineages that are prevalent in Turkey as well. However, the most prevalent sequence type in our study was ST2096. The majority of ST2096 strains were expressing the K1 capsule serotype (¾, 75%). This lineage is generally associated with MDR *K.pneumoniae* isolates. (Hosbul et al., 2021) This clone is the most common MDR *K.pneumoniae* clone in Turkey. (Isler et al., 2022) The high prevalence of ST2096 clones

within the hypervirulent cohort (30%) may be the indicator of the convergence of MDR isolates to MDR-hvKp strains by harboring both antimicrobial resistance and virulence plasmids. (Shankar et al., 2022) The increase in colistin resistance in ST2096 clones emphasizes the risk of severe invasive infections with high treatment failure outcomes. (Isler et al., 2022)

The limitation of this study is the selection of isolates that contained a high ratio of MDR *K.pneumoniae* isolates. Also, the number of isolates from recent years was relatively low compared to the isolates from the early years. Having equal sample sizes for isolates with different AMR profiles and isolation years would give more accountable results. Another limitation is the constrained sample size for the macrophage infection experiment. Increasing the number of cKp, hgKp, and hvKp isolates for the infection would help to see the bigger picture of the hypervirulence pathogenesis mechanism. Also, pro-inflammatory cytokine secretion levels were only observed for 6 hours of infection. Considering that the 2-3 hours period is crucial for hvKp infection, not documenting the cytokine levels at the early stages of infection is a limitation of the study.

# Chapter 5

## CONCLUSION

Hypervirulent *K.pneumoniae* is an emerging pathogen, especially in some clones such as K1 capsule carrying ST2096, and ST23. Together with the increasing antimicrobial resistance, it is a serious concern in our region just like in other parts of the world. The rapid convergence of MDR strains to MDR-hvKp will inevitably harden the treatment of infections. It is crucial to differentiate hypervirulent strains for efficient treatment, and the *peg344* gene is an accurate biomarker for differentiation in this region. To evade the host's innate immune response is the strategy of hypervirulent clones. The hypophagia of macrophages and the suppressed proinflammatory responses in the early stages contributes to the severe infections caused by hypervirulent clones. The *peg344* gene plays an important role in bacteria's resistance against phagocytosis by macrophage cells.

# BIBLIOGRAPHY

Andreata, F., Blériot, C., Di Lucia, P., De Simone, G., Fumagalli, V., Ficht, X., Beccaria, C. G.,Kuka, M., Ginhoux, F., & Iannacone, M. (2021). Isolation of mouse Kupffer cells for phenotypic and functional studies. *STAR protocols*, *2*(4), 100831. https://doi.org/10.1016/j.xpro.2021.100831

Arakawa, Y., Wacharotayankun, R., Nagatsuka, T., Ito, H., Kato, N., & Ohta, M. (1995). Genomic organization of the *Klebsiella pneumoniae cps* region responsible for Serotype K2 capsular polysaccharide synthesis in the virulent strain Chedid. *Journal of bacteriology*, *177*(7), 1788–1796. https://doi.org/10.1128/jb.177.7.1788-1796.1995

Athamna, A., Ofek, I., Keisari, Y., Markowitz, S., Dutton, G. G., & Sharon, N. (1991). Lectinophagocytosis of encapsulated *Klebsiella pneumoniae* mediated by surface lectins of guinea pig alveolar macrophages and human monocyte-derived macrophages. *Infection and immunity*, *59*(5), 1673–1682. https://doi.org/10.1128/iai.59.5.1673-1682.1991

Bach, S., de Almeida, A., & Carniel, E. (2000). The Yersinia high-pathogenicity island is present in different members of the family Enterobacteriaceae. *FEMS microbiology letters*, *183*(2), 289–294. https://doi.org/10.1111/j.1574-6968.2000.tb08973.x

Bachman, M. A., Lenio, S., Schmidt, L., Oyler, J. E., & Weiser, J. N. (2012). Interaction Of lipocalin 2, transferrin, and siderophores determines the replicative niche of *Klebsiella pneumoniae* during pneumonia. *mBio*, *3*(6), e00224-11. https://doi.org/10.1128/mBio.00224-11

Brisse S, Fevre C, Passet V, Issenhuth-Jeanjean S, Tournebize R, et al. (2009) Virulent Clones of *Klebsiella pneumoniae*: Identification and Evolutionary Scenario Based on Genomic and Phenotypic Characterization. PLoS ONE 4(3): e4982. doi:10.1371/journal.pone.0004982

Bulger, J., MacDonald, U., Olson, R., Beanan, J., & Russo, T. A. (2017). Metabolite Transporter PEG344 Is Required for Full Virulence of Hypervirulent *Klebsiella pneumoniae* Strain hvKP1 after Pulmonary but Not Subcutaneous Challenge. *Infection and immunity*, *85*(10), e00093-17. https://doi.org/10.1128/IAI.00093-17

Candan, E. D., & Aksöz, N. (2015). *Klebsiella pneumoniae*: characteristics of Carbapenem resistance and virulence factors. *Acta biochimica Polonica*, *62*(4), 867–874. https://doi.org/10.18388/abp.2015_1148

Catalán-Nájera JC, Garza-Ramos U, Barrios-Camacho H. (2017). Hypervirulence and hypermucoviscosity: Two different but complementary *Klebsiella* spp. phenotypes?, Virulence, 8:7, 1111-1123, https://doi.org/10.1080/21505594.2017.1317412

Chang, Angela Y., Chau, Vivian WY., Landas, Julius A., Pang, Yvonne. (2017). Preparation of calcium-competent *Escherichia coli* and heat-shock transformation. JEMI METHODS Vol. 1:22- 25

Chen, L., & Kreiswirth, B. N. (2018). Convergence of carbapenem-resistance and Hypervirulence in *Klebsiella pneumoniae*. *The Lancet. Infectious diseases*, *18*(1), 2–3. https://doi.org/10.1016/S1473-3099(17)30517-0

Cheng D, Liu Y, Yen M, Liu C, Wang R. (1991). Septic Metastatic Lesions of Pyogenic Liver Abscess: Their Association With *Klebsiella pneumoniae* Bacteremia in Diabetic Patients. *Arch Intern Med.* 1991;151(8):1557–1559. https://doi.org/10.1001/archinte.1991.00400080059010

Cheng NC, Yu YC, Tai HC, Hsueh PR, Chang SC, Lai SY, Yi SY, Fang CT. (2012). Recent Trend of Necrotizing Fasciitis in Taiwan: Focus on Monomicrobial *Klebsiella pneumoniae* Necrotizing Fasciitis, *Clinical Infectious Diseases*, Volume 55, Issue 7, 1 October 2012, Pages 930–939, https://doi.org/10.1093/cid/cis565

Chung, D. R., Lee, S. S., Lee, H. R., Kim, H. B., Choi, H. J., Eom, J. S., Kim, J. S., Choi, Y. H., Lee, J. S., Chung, M. H., Kim, Y. S., Lee, H., Lee, M. S., Park, C. K., & Korean Study Group for Liver Abscess. (2007). Emerging invasive liver abscess caused by K1 serotype *Klebsiella pneumoniae* in Korea. *The Journal of infection*, *54*(6), 578–583. https://doi.org/10.1016/j.jinf.2006.11.008

Compain F, Babosan A, Brisse S, Genel N, Audo J, Ailloud F, Kassis-Chikhani N, Arlet G, Decré D. (2014). Multiplex PCR for detection of seven virulence factors and K1/K2 capsular serotypes of *Klebsiella pneumoniae*. J Clin Microbiol. 2014 Dec;52(12):4377-80. https://doi.org/10.1128/JCM.02316-14. Epub 2014 Oct 1. PMID: 25275000; PMCID: PMC4313302.

Datsenko, K. A., & Wanner, B. L. (2000). One-step inactivation of chromosomal genes In *Escherichia coli* K-12 using PCR products. *Proceedings of the National Academy of Sciences of the United States of America*, *97*(12), 6640–6645. https://doi.org/10.1073/pnas.120163297

Diagnostic Restriction Digest. Addgene (2018, May). https://www.addgene.org/protocols/diagnostic-digest/. Retrieval Date: 28.06.2023

Diancourt L, Passet V, Verhoef J, Grimont PA, Brisse S. (2005). Multilocus sequence Typing of *Klebsiella pneumoniae* nosocomial isolates. J Clin Microbiol. 2005 Aug;43(8):4178-82. https://doi.org/10.1128/JCM.43.8.4178-4182.2005. PMID: 16081970; PMCID: PMC1233940.

Dogan O, Vatansever C, Atac N, Albayrak O, Karahuseyinoglu S, Sahin OE, Kilicoglu BK, Demiray A, Ergonul O, Gönen M, Can F. Virulence Determinants of Colistin-Resistant *K. pneumoniae* High-Risk Clones. Biology (Basel). 2021 May 14;10(5):436. https://doi.org/10.3390/biology10050436. PMID: 34068937; PMCID: PMC8155863.

Du, Q., Pan, F., Wang, C., Yu, F., Shi, Y., Liu, W., Li, Z., He, P., Han, D., & Zhang, H. (2022). Nosocomial dissemination of hypervirulent *Klebsiella pneumoniae* with high-risk clones among children in Shanghai. *Frontiers in cellular and infection microbiology*, *12*, 984180. https://doi.org/10.3389/fcimb.2022.984180

El Fertas-Aissani, R., Messai, Y., Alouache, S., & Bakour, R. (2013). Virulence profiles and antibiotic susceptibility patterns of *Klebsiella pneumoniae* strains isolated from different clinical specimens. *Pathologie-biologie*, *61*(5), 209–216. https://doi.org/10.1016/j.patbio.2012.10.004

Fang CT, Chuang YP, Shun CT, Chang SC, Wang JT. (2004). A novel virulence gene in *Klebsiella pneumoniae* strains causing primary liver abscess and septic Metastatic complications. J Exp Med. 2004 Mar 1;199(5):697-705. doi: 10.1084/jem.20030857. PMID: 14993253; PMCID: PMC2213305.

Fang, C. T., Lai, S. Y., Yi, W. C., Hsueh, P. R., & Liu, K. L. (2010). The function of wzy_K1(magA), the serotype K1 polymerase gene in *Klebsiella pneumoniae cps* gene cluster. *The Journal of infectious diseases*, *201*(8), 1268–1269. https://doi.org/10.1086/652183

Follador, R., Heinz, E., Wyres, K. L., Ellington, M. J., Kowarik, M., Holt, K. E., & Thomson, N. R. (2016). The diversity of *Klebsiella pneumoniae* surface polysaccharides. *Microbial genomics*, *2*(8), e000073. https://doi.org/10.1099/mgen.0.000073

Fung, C. P., Chang, F. Y., Lee, S. C., Hu, B. S., Kuo, B. I., Liu, C. Y., Ho, M., & Siu, L. K. (2002). A global emerging disease of *Klebsiella pneumoniae* liver abscess: is serotype K1 an important factor for complicated endophthalmitis?. *Gut*, *50*(3), 420–424. https://doi.org/10.1136/gut.50.3.420

Gu, D., Dong, N., Zheng, Z., Lin, D., Huang, M., Wang, L., Chan, E. W., Shu, L., Yu, J., Zhang, R., & Chen, S. (2018). A fatal outbreak of ST11 carbapenem-resistant Hypervirulent *Klebsiella pneumoniae* in a Chinese hospital: a molecular epidemiological study. *The Lancet. Infectious diseases*, *18*(1), 37–46. https://doi.org/10.1016/S1473-3099(17)30489-9

Hallal Ferreira Raro, O., Nordmann, P., Dominguez Pino, M., Findlay, J., & Poirel, L. (2023). Emergence of Carbapenemase-Producing Hypervirulent *Klebsiella pneumoniae* in Switzerland. *Antimicrobial agents and chemotherapy*, *67*(3), E0142422. https://doi.org/10.1128/aac.01424-22

Harada, S., & Doi, Y. (2018). Hypervirulent *Klebsiella pneumoniae*: a Call for Consensus Definition and International Collaboration. *Journal of clinical microbiology*, *56*(9), e00959-18. https://doi.org/10.1128/JCM.00959-18

Holden, V. I., Lenio, S., Kuick, R., Ramakrishnan, S. K., Shah, Y. M., & Bachman, M. A. (2014). Bacterial siderophores that evade or overwhelm lipocalin 2 induce hypoxia inducible factor 1α and proinflammatory cytokine secretion in cultured respiratory epithelial cells. *Infection and immunity*, *82*(9), 3826–3836. https://doi.org/10.1128/IAI.01849-14

Holmes, M. A., Paulsene, W., Jide, X., Ratledge, C., & Strong, R. K. (2005). Siderocalin (Lcn 2) also binds carboxymycobactins, potentially defending against mycobacterial infections through iron sequestration. *Structure (London, England : 1993)*, *13*(1), 29–41. https://doi.org/10.1016/j.str.2004.10.009

Hosbul, T., Guney-Kaya, K., Guney, M., Sakarya, S., Bozdogan, B., & Oryasin, E. (2021). Carbapenem and Colistin Resistant *Klebsiella Pneumoniae* ST14 and ST2096 Dominated in Two Hospitals in Turkey. *Clinical laboratory*, *67*(9), 10.7754/Clin.Lab.2021.201226. https://doi.org/10.7754/Clin.Lab.2021.201226

Hossain MJ, Thurlow CM, Sun D, Nasrin S, Liles MR. (2015). Genome modifications And cloning using a conjugally transferable recombineering system. Biotechnol Rep (Amst). 2015 Aug 28;8:24-35. https://doi.org/10.1016/j.btre.2015.08.005. PMID: 28352570; PMCID: PMC4980705.

Hsieh, P. F., Lin, T. L., Lee, C. Z., Tsai, S. F., & Wang, J. T. (2008). Serum-induced iron-acquisition systems and TonB contribute to virulence in *Klebsiella pneumoniae* causing primary pyogenic liver abscess. *The Journal of infectious diseases*, *197*(12), 1717–1727. https://doi.org/10.1086/588383

Isler, B., Özer, B., Çınar, G., Aslan, A. T., Vatansever, C., Falconer, C., Dolapçı, İ., Şimşek, F., Tülek, N., Demirkaya, H., Menekşe, Ş., Akalin, H., Balkan, İ. İ., Aydın, M., Tigen, E. T., Demir, S. K., Kapmaz, M., Keske, Ş., Doğan, Ö., Arabacı, Ç., … Ergönül, Ö. (2022). Characteristics and outcomes of carbapenemase harboring carbapenem-resistant Klebsiella spp. bloodstream infections: a multicentre prospective cohort study in an OXA-48 endemic setting. *European journal of clinical microbiology & infectious diseases : official publication of the European Society of Clinical Microbiology*, *41*(5), 841–847. https://doi.org/10.1007/s10096-022-04425-4

Jung J, Park KH, Park SY, Song EH, Lee EJ, Choi SH, Choo EJ, Kwak YG, Sung H, Kim SH, Lee SO, Kim MN, Kim YS, Woo JH, Choi SH. (2015). Comparison of The clinical characteristics and outcomes of *Klebsiella pneumoniae* and meningitis, Diagnostic Microbiology and Infectious Disease, Volume 82, Issue 1, 2015, Pages 87-91,ISSN 0732-8893, https://doi.org/10.1016/j.diagmicrobio.2015.02.006.

Kabha, K., Nissimov, L., Athamna, A., Keisari, Y., Parolis, H., Parolis, L. A., Grue, R. M., Schlepper-Schafer, J., Ezekowitz, A. R., & Ohman, D. E. (1995). Relationships among capsular structure, phagocytosis, and mouse virulence in *Klebsiella pneumoniae*. *Infection and immunity*, *63*(3), 847–852. https://doi.org/10.1128/iai.63.3.847-852.1995

Kuş, H., Arslan, U., Türk Dağı, H., & Fındık, D. (2017). Hastane enfeksiyonu etkeni *Klebsiella pneumoniae* izolatlarında çeşitli virülans faktörlerinin araştırılması [Investigation of various virulence factors of *Klebsiella pneumoniae* strains isolated from nosocomial infections]. *Mikrobiyoloji bülteni*, *51*(4), 329–339. https://doi.org/10.5578/mb.59716

Lee, H. C., Chuang, Y. C., Yu, W.L., Lee, N. Y., Chang, C. M., KO, N. Y., Wang, L. R. and Ko, W. C. (2006). Clinical implications of hypermucoviscosity phenotype in *Klebsiella pneumoniae* isolates: association with invasive syndrome in patients With community-acquired bacteraemia. Journal of Internal Medicine, 259: 606-614. https://doi.org/10.1111/j.1365-2796.2006.01641.x

Lee, C. H., Chang, C. C., Liu, J. W., Chen, R. F., & Yang, K. D. (2014). Sialic acid involved in hypermucoviscosity phenotype of *Klebsiella pneumoniae* and associated with resistance to neutrophil phagocytosis. *Virulence*, *5*(6), 673–679. https://doi.org/10.4161/viru.32076

Lee, C. H., Chuah, S. K., Chang, C. C., & Chen, F. J. (2020). The Surface Protein Fructose-1, 6 Bisphosphate Aldolase of *Klebsiella pneumoniae* Serotype K1: Role of Interaction with Neutrophils. *Pathogens (Basel, Switzerland)*, *9*(12), 1009. https://doi.org/10.3390/pathogens9121009

Lee, C. R., Lee, J. H., Park, K. S., Jeon, J. H., Kim, Y. B., Cha, C. J., Jeong, B. C., & Lee, S. H. (2017). Antimicrobial Resistance of Hypervirulent *Klebsiella Pneumoniae*: Epidemiology, Hypervirulence-Associated Determinants, and Resistance Mechanisms. *Frontiers in cellular and infection microbiology*, *7*, 483. https://doi.org/10.3389/fcimb.2017.00483

Li, G., Shi, J., Zhao, Y., Xie, Y., Tang, Y., Jiang, X., & Lu, Y. (2020). Identification of hypervirulent *Klebsiella pneumoniae* isolates using the string test in combination With *Galleria mellonella* infectivity. *European journal of clinical microbiology & infectious diseases : official publication of the European Society of Clinical Microbiology*, *39*(9), 1673–1679. https://doi.org/10.1007/s10096-020-03890-z

Li, P., Peng, T., Xiang, T., Luo, W., Liao, W., Wei, D. D., Luo, S., He, Z., Liu, P., Zhang, W., & Liu, Y. (2023). *Klebsiella pneumoniae* outer membrane vesicles induce strong IL-8 expression via NF-κB activation in normal pulmonary bronchial cells. *International immunopharmacology*, *121*, 110352. Advance online publication. https://doi.org/10.1016/j.intimp.2023.110352

Liu, Y. C., Cheng, D. L., & Lin, C. L. (1986). *Klebsiella pneumoniae* liver abscess associated with septic endophthalmitis. *Archives of internal medicine*, *146*(10), 1913–1916.

Melot B, Brisse S, Breurec S, Passet V, Malpote E, Lamaury I, Thiery G, Hoen B. (2016). Community-acquired meningitis caused by a CG86 hypervirulent *Klebsiella pneumoniae* strain: first case report in the Caribbean. BMC Infect Dis. 2016 Dec 7;16(1):736. doi: 10.1186/s12879-016-2065-2. PMID: 27923372; PMCID: PMC5142283.

Moellering, R. C. (2010). NDM-1 — A Cause for Worldwide Concern. *The New England Journal of Medicine*, *363*(25), 2377–2379. https://doi.org/10.1056/nejmp1011715

Moyes, R. B., Reynolds, J., & Breakwell, D. P. (2009). Preliminary staining of bacteria: Negative stain. *Current protocols in microbiology*, *Appendix 3*,. https://doi.org/10.1002/9780471729259.mca03fs15

Murdoch, C. C., & Skaar, E. P. (2022). Nutritional immunity: the battle for nutrient metals at the host-pathogen interface. *Nature reviews. Microbiology*, *20*(11), 657–670. https://doi.org/10.1038/s41579-022-00745-6

Nassif, X., & Sansonetti, P. J. (1986). Correlation of the virulence of *Klebsiella pneumoniae* K1 and K2 with the presence of a plasmid encoding aerobactin. *Infection and immunity*, *54*(3), 603–608. https://doi.org/10.1128/iai.54.3.603-608.1986

Nicolò, S., Mattiuz, G., Antonelli, A., Arena, F., Di Pilato, V., Giani, T., Baccani, I., Clemente, A. M., Castronovo, G., Tanturli, M., Cozzolino, F., Rossolini, G. M., & Torcia, M. G. (2022). Hypervirulent *Klebsiella pneumoniae* Strains Modulate Human Dendritic Cell Functions and Affect TH1/TH17 Response. *Microorganisms*, *10*(2), 384. https://doi.org/10.3390/microorganisms10020384

Ombada, M., Perwez, T., Campitelli, M., & Zeineddine, N. (2023). Hypermucoviscous *Klebsiella pneumoniae*: A Hypervirulent Strain Masquerading as Metastasis. *Cureus*, *15*(5), e39561. https://doi.org/10.7759/cureus.39561

Örsten, S., Demirci-Duarte, S., Ünalan-Altıntop, T., Çakar, A., Sancak, B., Ergünay, K., & Özkuyumcu, C. (2020). Low prevalence of hypervirulent *Klebsiella pneumoniae* in Anatolia, screened via phenotypic and genotypic testing. *Acta microbiologica et immunologica Hungarica*, *67*(2), 120–126. https://doi.org/10.1556/030.2020.01143

Paczosa MK, Mecsas J. (2016). *Klebsiella pneumoniae*: going on the offense with a Strong Defense, Microbiol Mol Biol Rev 80:629 - 661. https://doi.org/10.1128/MMBR.00078-15.

Pei, N., Liu, X., Jian, Z., Yan, Q., Liu, Q., Kristiansen, K., Li, J., & Liu, W. (2023). Genome sequence and genomic analysis of liver abscess caused by hypervirulent *Klebsiella pneumoniae*. *3 Biotech*, *13*(3), 76. https://doi.org/10.1007/s13205-023-03458-6

Peirano, G., Pitout, J. D., Laupland, K. B., Meatherall, B., & Gregson, D. B. (2013). Population-based surveillance for hypermucoviscosity *Klebsiella pneumoniae* causing community-acquired bacteremia in Calgary, Alberta. *The Canadian journal of infectious diseases & medical microbiology = Journal canadien des maladies infectieuses et de la microbiologie medicale*, *24*(3), e61–e64. https://doi.org/10.1155/2013/828741

Pereira, S. C., & Vanetti, M. C. (2015). Potential virulence of *Klebsiella* sp. Isolates from enteral diets. *Brazilian journal of medical and biological research*, *48*(9), 782–789. https://doi.org/10.1590/1414-431X20154316

Phuong MS, Hernandez RE, Wolter DJ, Hoffman LR, Sad S. (2021). Impairment in inflammasome signaling by the chronic *Pseudomonas aeruginosa* isolates from Cystic fibrosis patients results in an increase in inflammatory response. Cell Death Dis. 2021 Mar 4;12(3):241.https://doi.org/10.1038/s41419-021-03526-w. PMID: 33664232; PMCID: PMC7933143.

Pinney, J. J., Rivera-Escalera, F., Chu, C. C., Whitehead, H. E., VanDerMeid, K. R., Nelson, A. M., Barbeau, M. C., Zent, C. S., & Elliott, M. R. (2020). Macrophage hypophagia as a mechanism of innate immune exhaustion in mAb-induced cell clearance. *Blood*, *136*(18), 2065–2079. https://doi.org/10.1182/blood.2020005571

Prokesch, B. C., TeKippe, M., Kim, J., Raj, P., TeKippe, E. M., & Greenberg, D. E. (2016). Primary osteomyelitis caused by hypervirulent *Klebsiella pneumoniae*. The Lancet Infectious Diseases, 16(9), e190–e195. https://doi.org/10.1016/s1473-3099(16)30021-4

Raymond, K. N., Dertz, E. A., & Kim, S. S. (2003). Enterobactin: an archetype for Microbial iron transport. *Proceedings of the National Academy of Sciences of the United States of America*, *100*(7), 3584–3588. https://doi.org/10.1073/pnas.0630018100

Russo, T. A., & Marr, C. M. (2019). Hypervirulent Klebsiella pneumoniae. *Clinical Microbiology Reviews*, *32*(3). https://doi.org/10.1128/cmr.00001-19

Russo, T. A., Olson, R., MacDonald, U., Beanan, J., & Davidson, B. A. (2015). Aerobactin, but not yersiniabactin, salmochelin, or enterobactin, enables the growth/survival of hypervirulent (hypermucoviscous) *Klebsiella pneumoniae* ex vivo and in vivo. *Infection and immunity*, *83*(8), 3325–3333. https://doi.org/10.1128/IAI.00430-15

Russo, T. A., Olson, R., Fang, C. T., Stoesser, N., Miller, M., MacDonald, U., Hutson, A., Barker, J. H., La Hoz, R. M., & Johnson, J. R. (2018). Identification of Biomarkers for Differentiation of Hypervirulent *Klebsiella pneumoniae* from Classical *K.pneumoniae. Journal of clinical microbiology*, *56*(9), e00776-18. https://doi.org/10.1128/JCM.00776-18

Russo, T. A., Olson, R., Macdonald, U., Metzger, D., Maltese, L. M., Drake, E. J., & Gulick, A. M. (2014). Aerobactin mediates virulence and accounts for increased Siderophore production under iron-limiting conditions by hypervirulent (hypermucoviscous) *Klebsiella pneumoniae*. *Infection and immunity*, *82*(6), 2356–2367. https://doi.org/10.1128/IAI.01667-13

Russo, T. A., MacDonald, U., Hassan, S., Camanzo, E., LeBreton, F., Corey, B., & McGann, P. (2021). An Assessment of Siderophore Production, Mucoviscosity, and Mouse Infection Models for Defining the Virulence Spectrum of Hypervirulent *Klebsiella pneumoniae*. *mSphere*, *6*(2), e00045-21. https://doi.org/10.1128/mSphere.00045-21

Sahly, H., Aucken, H., Benedi, V. J., Forestier, C., Fussing, V., Hansen, D. S., Ofek, I., Podschun, R., Sirot, D., Sandvang, D., Tomás, J. M., & Ullmann, U. (2004). Impairment of respiratory burst in polymorphonuclear leukocytes by Extended-spectrum beta-lactamase-producing strains of *Klebsiella pneumoniae. European journal of clinical microbiology & infectious diseases : official publication of the European Society of Clinical Microbiology*, *23*(1), 20–26. https://doi.org/10.1007/s10096-003-1047-7

Sahly, H., Keisari, Y., Crouch, E., Sharon, N., & Ofek, I. (2008). Recognition of bacterial surface polysaccharides by lectins of the innate immune system and its contribution to defense against infection: the case of pulmonary pathogens. *Infection and immunity*, *76*(4), 1322–1332. https://doi.org/10.1128/IAI.00910-07

Sánchez-Diener I, Zamorano L, López-Causapé C, Cabot G, Mulet X, Peña C, del Campo R, Cantón R, Doménech-Sánchez A, Martínez-Martínez L, Arcos SC, Navas A, Oliver A. (2017). Interplay among resistance profiles, high-risk clones,

and virulence in the *Caenorhabditis elegans Pseudomonas aeruginosa* infection model. Antimicrob Agents Chemother 61:e01586-17. https://doi.org/10.1128/AAC.01586-17 .

Sánchez-López J, García-Caballero A, Navarro-San Francisco C, Quereda C, Ruiz-Garbajosa P, Navas E, Dronda F, Morosini MI, Cantón R, Diez-Aguilar M. (2019). Hypermucoviscous *Klebsiella pneumoniae*: A challenge in community Acquired infection. IDCases. 2019 May 3;17:e00547. https://doi.org/10.1016/j.idcr.2019.e00547. PMID: 31193033; PMCID: PMC6514362.

Schubert, S., Cuenca, S., Fischer, D., & Heesemann, J. (2000). High-pathogenicity island of *Yersinia pestis* in Enterobacteriaceae isolated from blood cultures and urine samples: prevalence and functional expression. *The Journal of infectious diseases*, *182*(4), 1268–1271. https://doi.org/10.1086/315831

Shankar, C., Vasudevan, K., Jacob, J. J., Baker, S., Isaac, B. J., Neeravi, A. R., Sethuvel, D. P. M., George, B., & Veeraraghavan, B. (2022). Hybrid Plasmids Encoding Antimicrobial Resistance and Virulence Traits Among Hypervirulent *Klebsiella pneumoniae* ST2096 in India. *Frontiers in cellular and infection microbiology*, *12*, 875116.https://doi.org/10.3389/fcimb.2022.875116

Shen, P., Berglund, B., Chen, Y., Zhou, Y., Xiao, T., Xiao, Y., & Zhou, K. (2020). Hypervirulence Markers Among Non-ST11 Strains of Carbapenem- and Multidrug-Resistant *Klebsiella pneumoniae* Isolated From Patients With Bloodstream Infections. *Frontiers in microbiology*, *11*, 1199. https://doi.org/10.3389/fmicb.2020.01199

Shi SH, Feng XN, Lai MC, Kong HS, Zheng SS. (2017). Biliary diseases as main causes of pyogenic liver abscess caused by extended-spectrum Beta-lactamase-producing Enterobacteriaceae. Liver Int. 2017 May;37(5):727-734. https://doi.org/10.1111/liv.13267. Epub 2016 Oct 29. PMID: 27718321.

Shi Q, Lan P, Huang D, Hua X, Jiang Y, Zhou J, Yu Y. (2018). Diversity of virulence level phenotype of hypervirulent *Klebsiella pneumoniae* from different sequence type lineage. BMC Microbiol 18:94. https://doi.org/10 .1186/s12866-018-1236-2

Shon, A. S., & Russo, T. A. (2012). Hypervirulent *Klebsiella pneumoniae:* the next Superbug? *Future Microbiology*, *7*(6), 669–671. https://doi.org/10.2217/fmb.12.43

Struve, C., Roe, C. C., Stegger, M., Stahlhut, S. G., Hansen, D. S., Engelthaler, D. M., Andersen, P. S., Driebe, E. M., Keim, P., & Krogfelt, K. A. (2015). Mapping the Evolution of Hypervirulent *Klebsiella pneumoniae*. *mBio*, *6*(4), e00630. https://doi.org/10.1128/mBio.00630-15

Tian, C., Shi, Y., Ren, L., Huang, D., Wang, S., Zhao, Y., Fu, L., Bai, Y., Xia, D., & Fan, X. (2023). Emergence of IS26-mediated pLVPK-like virulence and NDM-1 Conjugative fusion plasmid in hypervirulent carbapenem-resistant *Klebsiella pneumoniae. Infection, genetics and evolution : journal of molecular epidemiology and evolutionary genetics in infectious diseases*, *113*, 105471. Advance online publication. https://doi.org/10.1016/j.meegid.2023.105471

Turton JF, Baklan H, Siu LK, Kaufmann ME, Pitt TL. (2008). Evaluation of a multiplex PCR for detection of serotypes K1, K2 and K5 in Klebsiella sp. and comparison of isolates within these serotypes. FEMS Microbiol Lett. 2008 Jul;284(2):247-52. https://doi.org/10.1111/j.1574-6968.2008.01208.x. Epub 2008 May 27. PMID: 18507682.

Turton JF, Payne Z, Coward A, Hopkins KL, Turton JA, Doumith M, Woodford N. (2016). Virulence genes in isolates of *Klebsiella pneumoniae* from the UK during 2016, including among carbapenemase gene-positive hypervirulent K1-ST23 and 'non-hypervirulent' types ST147, ST15 and ST383. J Med Microbiol. 2018 Jan;67(1):118-128. https://doi.org/10.1099/jmm.0.000653. Epub 2017 Dec 5. PMID: 29205138.

Wanford, J. J., Hames, R. G., Carreno, D., Jasiunaite, Z., Chung, W. Y., Arena, F., Di Pilato, V., Straatman, K., West, K., Farzand, R., Pizza, M., Martinez-Pomares, L., Andrew, P. W., Moxon, E. R., Dennison, A. R., Rossolini, G. M., & Oggioni, M. R. (2021). Interaction of *Klebsiella pneumoniae* with tissue macrophages in a mouse infection model and ex-vivo pig organ perfusions: an exploratory investigation. *The Lancet. Microbe*, *2*(12), e695–e703. https://doi.org/10.1016/S2666-5247(21)00195-6

Wang, G., Zhao, G., Chao, X., Xie, L., & Wang, H. (2020). The Characteristics of Virulence, Biofilm and Antibiotic Resistance of *Klebsiella pneumoniae*. *International journal of environmental research and public health*, *17*(17), 6278. https://doi.org/10.3390/ijerph17176278

Wang JH, Liu YC, Lee SSJ, Yen MY, Chen YS, Wang JH. (1998). Primary Liver Abscess Due to *Klebsiella pneumoniae* in Taiwan, *Clinical Infectious Diseases*, Volume 26, Issue 6, Pages 1434–1438, https://doi.org/10.1086/516369

Wu, Y., Wu, C., Bao, D., Jia, H., Draz, M. S., He, F., & Ruan, Z. (2022). Global evolution and geographic diversity of hypervirulent carbapenem-resistant *Klebsiella pneumoniae*. *The Lancet. Infectious diseases*, *22*(6), 761–762. https://doi.org/10.1016/S1473-3099(22)00275-4

Wyres, K. L., Lam, M. M. C., & Holt, K. E. (2020). Population genomics of *Klebsiella pneumoniae*. *Nature reviews. Microbiology*, *18*(6), 344–359. https://doi.org/10.1038/s41579-019-0315-1

Yu, W. L., Ko, W. C., Cheng, K. C., Lee, H. C., Ke, D. S., Lee, C. C., Fung, C. P., & Chuang, Y. C. (2006). Association between *rmpA* and *magA* genes and clinical syndromes caused by *Klebsiella pneumoniae* in Taiwan. *Clinical infectious diseases : an official publication of the Infectious Diseases Society of America*, *42*(10), 1351–1358. https://doi.org/10.1086/503420

Yu, W. L., Ko, W. C., Cheng, K. C., Lee, C. C., Lai, C. C., & Chuang, Y. C. (2008). Comparison of prevalence of virulence factors for *Klebsiella pneumoniae* liver abscesses between isolates with capsular K1/K2 and non-K1/K2 serotypes.

*Diagnostic microbiology and infectious disease*, *62*(1), 1–6. https://doi.org/10.1016/j.diagmicrobio.2008.04.007

Zamani, A., Yousefi Mashouf, R., Ebrahimzadeh Namvar, A. M., & Alikhani, M. Y. (2013). Detection of magA Gene in Klebsiella spp. Isolated from Clinical Samples Detection of magA. *Iranian journal of basic medical sciences*, *16*(2), 173–176.

Zhang, R., Lin, D., Chan, E. D., Gu, D., Chen, G., & Chen, S. (2016). Emergence of Carbapenem-Resistant Serotype K1 Hypervirulent *Klebsiella pneumoniae* Strains in China. *Antimicrobial Agents and Chemotherapy*, *60*(1), 709–711. https://doi.org/10.1128/aac.02173-15

Zhu, J., Wang, T., Chen, L., & Du, H. (2021). Virulence Factors in Hypervirulent *Klebsiella pneumoniae*. *Frontiers in microbiology*, *12*, 642484. https://doi.org/10.3389/fmicb.2021.642484

Zou, H., Zhou, Z., Berglund, B., Zheng, B., Meng, M., Zhao, L., Zhang, H., Wang, Z., Wu, T., Li, Q., & Li, X. (2023). Persistent transmission of carbapenem-resistant, hypervirulent *Klebsiella pneumoniae* between a hospital and urban aquatic environments. *Water research*, *242*, 120263. Advance online publication. https://doi.org/10.1016/j.watres.2023.120263